Pedestrian Behavior Study to Advance Pedestrian Safety in Smart Transportation Systems Using Innovative LIDAR Sensors

Pengfei (Taylor) Li, Ph.D.
Sirisha Kothuri, Ph.D.
Katherine Keeling, MEng
Xianfeng (Terry) Yang, Ph.D.

UNIVERSITY OF TEXAS ARLINGTON

Portland State UNIVERSITY

THE UNIVERSITY OF UTAH

PEDESTRIAN BEHAVIOR STUDY TO ADVANCE PEDESTRIAN SAFETY IN SMART TRANSPORTATION SYSTEMS USING INNOVATIVE LIDAR SENSORS

Final Report

NITC-RR-1393

by

Pengfei (Taylor) Li
University of Texas at Arlington

Sirisha Kothuri
Katherine Keeling
Portland State University

Xianfeng (Terry) Yang
University of Utah

for

March 2023

Technical Report Documentation Page

1. Report No. NITC-RR-1393	2. Government Accession No.	3. Recipient's Catalog No.

4. Title and Subtitle
   Pedestrian Behavior Study to Advance Pedestrian Safety in Smart Transportation Systems Using Innovative LiDAR Sensors
		5. Report Date
		  March 2023

		6. Performing Organization Code

7. Author(s)
   Taylor Li (U of Texas at Arlington), 0000-0002-3833-5354
   Sirisha Kothuri, Katherine Keeling (PSU), 0000-0002-2952-169X
   Xianfeng (Terry) Yang (U of Utah), 0000-0002-9416-6882
   Farzana R. Chowdhury (U of Texas at Arlington)
		8. Performing Organization Report No.

9. Performing Organization Name and Address 425 Nedderman Hall, 416 Yates St., Box 19308, Arlington, TX 76019		10. Work Unit No. (TRAIS)
		11. Contract or Grant No. 69A3551747112

12. Sponsoring Agency Name and Address
 	
  U.S. Department of Transportation
  Office of the Assistant Secretary for Research and Technology
  1200 New Jersey Avenue, SE, Washington, DC 20590
		13. Type of Report and Period Covered
		Final Report

		14. Sponsoring Agency Code

16. Abstract

Pedestrian safety is critical to improving walkability in cities. Although walking trips have increased in the last decade, pedestrian safety remains a top concern. In 2020, 6,516 pedestrians were killed in traffic crashes, representing the most deaths since 1990 (NHTSA, 2020). Approximately 15% of these occurred at signalized intersections where a variety of modes converge, leading to the increased propensity of conflicts. Current signal timing and detection technologies are heavily biased towards vehicular traffic, often leading to higher delays and insufficient walk times for pedestrians, which could result in risky behaviors such as noncompliance. Current detection systems for pedestrians at signalized intersections consist primarily of push buttons. Limitations include the inability to provide feedback to the pedestrian that they have been detected, especially with older devices, and not being able to dynamically extend the walk times if the pedestrians fail to clear the crosswalk. Smart transportation systems play a vital role in enhancing mobility and safety and provide innovative techniques to connect pedestrians, vehicles, and infrastructure. Most research on smart and connected technologies is focused on vehicles; however, there is a critical need to harness the power of these technologies to study pedestrian behavior, as pedestrians are the most vulnerable users of the transportation system. While a few studies have used location technologies to detect pedestrians, this coverage is usually small and favors people with smartphones. However, the transportation system must consider a full spectrum of pedestrians and accommodate everyone.

In this research, the investigators first review the previous studies on pedestrian behavior data and sensing technologies. Then the research team developed a pedestrian behavioral data collecting system based on the emerging LiDAR sensors. The system was deployed at two signalized intersections. Two studies were conducted: (a) pedestrian behaviors study at signalized intersections, analyzing the pedestrian waiting time before crossing, generalized perception-reaction time to WALK sign and crossing speed; and (b) a novel dynamic flashing yellow arrow (D-FYA) solution to separate permissive left-turn vehicles from concurrent crossing pedestrians. The results reveal that the pedestrian behaviors may have evolved compared with the recommended behaviors in the pedestrian facility design guideline (e.g., AASHTO's "Green Book"). The D-FYA solution was also evaluated on the cabinet-in-the-loop simulation platform and the improvements were promising. The findings in this study will advance the body of knowledge on equitable traffic safety, especially for pedestrian safety in the future.

17. Key Words
 	
  Pedestrians, Safety, LIDAR sensors
	18. Distribution Statement
	  No restrictions. Copies available from NITC:
	  www.nitc-utc.net		

19. Security Classification (of this report) Unclassified	20. Security Classification (of this page) Unclassified	21. No. of Pages 52	22. Price

ACKNOWLEDGEMENTS

DISCLAIMER

RECOMMENDED CITATION

Li, Pengfei (Taylor), Sirisha Kothuri, Katherine Keeling, Xianfeng (Terry) Yang. *Pedestrian Behavior Study to Advance Pedestrian Safety in Smart Transportation Systems Using Innovative LiDAR Sensors*. NITC-RR-1393. Portland, OR: Transportation Research and Education Center (TREC), 2023.

TABLE OF CONTENTS

EXECUTIVE SUMMARY

In this project, the investigators first reviewed the literature on pedestrian behaviors and various technologies to collect pedestrian data. It was concluded that the studies on pedestrian behaviors, especially at signalized intersections, have been rather limited in the past 20 years. Therefore, this research effort is needed to provide up-to-date information on this topic.

The research team then developed a pedestrian behavior data collecting system based on the LiDAR sensing technologies and then deployed at two intersections. After a few months of stabilization, the developed software could reliably collect pedestrian behaviors. The developed solution collected thousands of pedestrian behavioral samples at each intersection over many months. The data analysis shows that the ADA-compliant (audible) pedestrian push buttons can significantly reduce pedestrians' "Effective Perception-Reaction (E-P-R)" time, defined as pedestrians' perception-reaction time to the onset of WALK plus the walking time from the waiting area into the intersection.

The research team also explored a novel dynamic flashing yellow arrow mechanism (D-FYA) to solve the conflict between the permissive left-turn vehicles and concurrent crossing pedestrians. Based on pedestrians' presence and trajectories, the flashing yellow arrow will either start on time, be postponed, or cancelled with each cycle. The proposed D-FYA can improve pedestrian safety while maximizing the permissive left-turn capacity. The results in traffic signal simulation were promising.

The findings of this study can improve pedestrian safety at signalized intersections.

1.0 INTRODUCTION

The objectives of this research are to develop a pedestrian behavior analytics framework, and to prove the concept of a novel dynamic flashing yellow arrow (D-FYA) mechanism with LiDAR sensor at signalized intersections. The LiDAR sensors have been used in automated vehicles to identify surrounding vehicles and pedestrians. They used to be prohibitively expensive, but the price has dramatically reduced to a comparable range with the widely adopted video or radar detectors. The LiDAR sensors outperform video or radar sensors in many aspects such as slow object tracking and being able to work in adverse weather conditions. Meanwhile, current traffic research and detection technologies are primarily for vehicular traffic even though pedestrian safety has been a top issue for decades. Traffic signal control operations are heavily biased toward vehicular traffic as well. The pedestrian fatalities, surprisingly, have reached the highest in the past 40 years (over 7,000 pedestrian deaths in 2022). As such, it is critical to conduct a pedestrian behavior study now to provide the latest planning and operation guidelines for pedestrian facilities, especially at intersections. The findings from this research can also be applicable during pandemics and other natural disasters, where nonmotorized travel becomes more popular, and cities must adapt to quickly prioritize the active transportation modes.

Prior to the availability of LiDAR tracking sensors, many obstacles existed to prevent extensive investigations into a pedestrian-focused multimodal traffic control system. A major obstacle is the lack of reliable pedestrian detection devices. Although multiple techniques like video analytics have been examined, they turn out either to be not reliable in all conditions or unsuitable for large-scale applications. The lack of reliable, cost-effective sensing techniques also results in the slow development of a multimodal traffic control system. While the techniques for vehicular traffic are fast evolving, less improvement has been made to favor pedestrians.

The rest of the report is laid out as follows. The literature review is next, followed by the development of a dynamic flashing yellow arrow strategy for left-turning vehicles and pedestrian behavior study.

2.0 LITERATURE REVIEW

Pedestrian safety is a critical prerequisite to promoting walkability in cities. Pedestrians are vulnerable road users, suffering the greatest risk of personal harm while posing the least amount of risk to others. In the 21st century, transportation developments in the United States were largely focused towards making the driver's experience as expedient and frictionless as possible, while providing little protections or technological advancements for the needs of pedestrians (Gutfreund, 2004; Levinson and Krizek, 2008). Guides for traffic controls at intersections have been developed for stewarding safety since the 1930s (American Association of State Highway Officials and National Conference on Street and Highway Safety, 1935; Schad, 1935), but the occurrence of pedestrian fatalities occurring at intersections has remained relatively flat for the past two decades, with no strong upward or downward trends (Figure 1). Even more pressing is the fact that although traffic fatalities have generally been trending downwards, pedestrian deaths are representing an increasing portion of overall traffic fatalities (NHTSA, 2018).
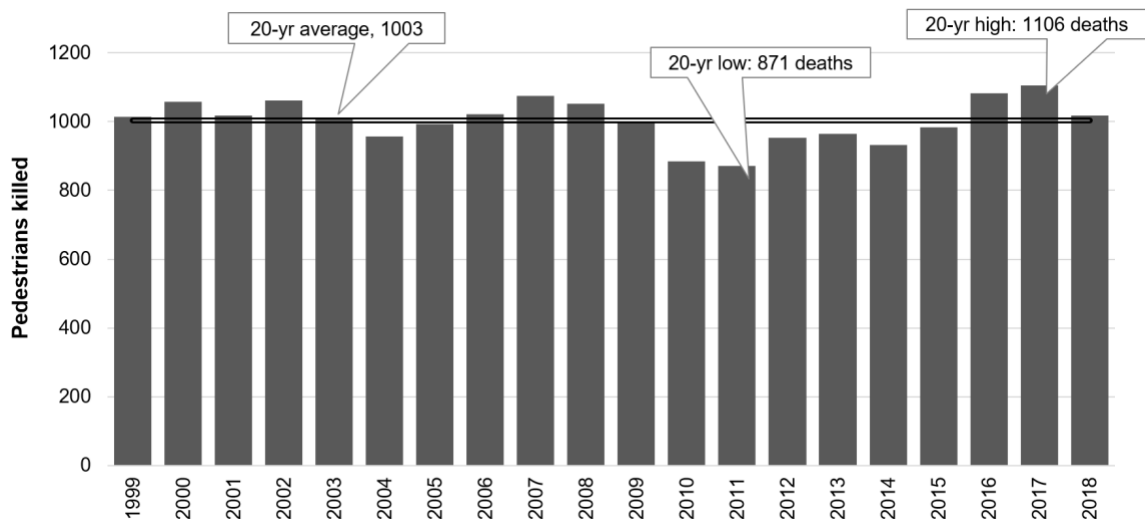
Figure 2.1: The last 20 years of pedestrians killed at intersections, annually, in the United States.

Some practitioners are promoting a "safe-systems approach" that embraces the need to design for naturally fallible, tired, distracted human road users as a foundational design

constraint (Grembek, 2019). Pedestrian deaths will decline when the man-made transportation system is redeveloped to suit the breadth of human behavior – for erroneous drivers and erroneous pedestrians. Past attempts to regulate a perpetual state of perfect travel behavior have fallen short. The motivation for this study is part of the broader shift from trying to control individual behavior to creating transportation systems that are not dangerous. Since the 1960s, inductive loop sensors have detected and facilitated motor vehicles (Klein et al., 2006), but pedestrian detection has been challenging due to variability in pedestrian walk/roll patterns and grouping arrangements, as well as the limits of sensor capability in wide environmental conditions including brightness and darkness; high and low temperatures; and rain, ice, and snow.

2.1 DEVELOPING SIGNAL TIMING TO SERVE PEDESTRIANS AT INTERSECTIONS

When the Manual of Uniform Traffic Control Devices (MUTCD) was first published in 1935, the United States had more fixed-time signals than traffic-actuated signals, but the authors hoped the efficiencies provided by traffic-actuated signals would better minimize delay and thus encourage more compliant behavior from drivers and pedestrians. Moreover, specific guidelines for signal timing had not yet been formalized, so the MUTCD offered heuristics for vehicular considerations and less-developed caveats regarding pedestrians. For example, for fixed-time signals, the timing of the yellow indication was tailored to vehicle clearance times and specified to be at least three seconds, unless the speeds were 35 mph or greater, in which they would be given at least five seconds (pg. 90). In contrast, pedestrian signals lacked a clearance phase indication (analogous to today's FLASHING DON'T WALK), and timed signals were considered to accommodate pedestrian clearance through a minimum green indication of at least 10 seconds, or a duration "sufficient to permit pedestrians to cross a point of safety (pg. 89)." Guidance was even less defined for traffic-actuated signals: "It is important…to consider the possibility of providing satisfactory pedestrian clearance periods under traffic-

actuated control (pg. 67)." As traffic volumes grew, the pedestrian-actuated push button was also recommended to create a break in traffic-actuated vehicle flow.

By the 1961 edition of the MUTCD, signal timing practices had developed and the MUTCD offered a standard for which to calculate pedestrian clearances: 4.0 feet per second was assumed to be the "normal walking pace (pg. 222)," with no empirical evidence cited. This pace and the width of the road would inform pedestrian signal timing. For roads with a median at least 4 feet wide, pedestrian clearances needed only be long enough to allow a pedestrian to reach the median. The implication is that it was deemed acceptable to require a pedestrian to take two cycles to cross the street.

However, the 1961 edition did standardize several signal-timing improvements for pedestrians: the addition of a FLASHING DON'T WALK signal to indicate when it was no longer appropriate to enter the crosswalk (pg. 221), and for pre-timed signals, the pedestrian clearance interval had to govern the minimum phase length. Additionally, the leading pedestrian phase was presented to create temporal distance between pedestrians and turning vehicles (pg. 222).

2.2 ACCOMODATING VARIABILITY IN PEDESTRIAN BEHAVIOR

The next big step for improving signals for pedestrians was passage of the Americans with Disabilities Act (1990), which established mobility in the public right of way as a civic right with legally enforceable requirements. It also paved the way for a broader "all ages and abilities" traffic design movement. Crash data clearly showed that adults ages 65-75 were disproportionately killed in crashes at intersections (Institute of Transportation Engineers, 2004). Researchers questioned the MUTCD's 4.0 feet/second assumed pedestrian pace used in calculating signal timing. Closer studies of those with mobility impairments showed that average walk paces varied quite considerably, from 2.1 ft/sec for walker users to 3.5 ft/sec for wheelchair users (Institute of Transportation Engineers, 1998).

2.2.1 Walk speeds for varying demographic groups and contexts

In the 2009 edition of the MUTCD, the recommended assumption for pedestrian travel was reduced to 3.5 ft/sec, which corresponds to the 15th percentile of expected walking speeds. These national guidelines have been further examined by different organizations and studies, with varying conclusions:

- In areas with high levels of seniors or people with mobility impairments, ITE has recommended the assumption of a walk speed of 2.5 ft/sec (Institute of Transportation Engineers, 2004).

- Other studies have or have supported the recommended 3.5 ft/sec (Hou et al., 2012).

- And other state-specific studies have found that the 15th percentile walk speed was slightly above 4.0 ft/sec (Schultz et al., 2019).

- Gender is also a strong predictor of walk speed, with female pedestrians demonstrating a slower walk time than males (Marisamynathan and Perumal, 2014).

These studies all posit a fixed pace to accommodate pedestrian needs. The drawbacks concomitant with assuming slower pedestrian walk rates are increases in the delay of stopped vehicles. Growing challenges of delay and congestion in growing cities produce serious economic and societal costs, but current intersection infrastructure (e.g., push button activation) does not have the capacity to accommodate varying walk speeds.

2.2.2 Pedestrian perception reaction time

Although careful deliberation has been given to the design walk to the 85th percentile walk speed, the mean perception reaction time has been used for pedestrian signal timing. The mean time required for pedestrian perception-reaction is 1.0 seconds, but the 85th percentile perception-reaction time is about 1.33 seconds (McGee et al., 2012). Although the final effects on signal timing decisions are small, using the mean perception reaction time does not factor in for the realities of individuals who are slower to respond to a WALK

signal, whether the slower reactions are attributable to cognitive impairments or distraction.

2.2.3 Push button activation – to minimize delay for pedestrians and tradeoffs

Since the 1930s, pedestrian actuation has been realized through the conscious intention of pedestrians pressing a push button. The fundamental design had not changed significantly until the development of accessible pedestrian signals (APS). In the accordance with the ADA, APS communicates to those with visual impairments through use of beaconing tones, auditory messaging, and tactile feedback (Barlow et al., 2003). Some offered an extended walk interval if the pedestrian pushed and held the button for three seconds. Studies found that 99% of pedestrians did not hold the button for three seconds, and 95% of pedestrians held the button for less than one second; the average hold time was 0.2 seconds (Noyce and Bentzen, 2005). Moreover, the buttons are designed to require five pounds of force and holding such force may be difficult for the very audience that would need the walk time extension (Barlow et al., 2003).

2.2.4 Automated pedestrian detection to supplement/replace push button activation

Rather than requiring the visually/mobility impaired to take another step for their safe crossing, the city of Adelaide, Australia, has required the installation of passive pedestrian detection for the purpose of extending crossing time for all new APS installations (Barlow et al., 2003). This example underscores the essential shift needed to apply developing a systems-safety approach to transportation networks: safety developments should be built into the system's operation, and not require anything more than on the part of compliant pedestrian behavior.

The United States has performed automated pedestrian detection trials at two intersections in Rochester, NY, and one intersection each in Phoenix, AZ, and Los Angeles, CA. They were installed to run in tandem with existing push button activation

systems, such that if a pedestrian did not push the button the automated sensor would provide the pedestrian-oriented activation. These trials found that pedestrians were less likely to begin crossing during DON'T WALK signals (χ^2= 6.019, df = 1, p = 0.014) when accommodated by passive detection (Hughes et al., 2001).

2.2.5 Dynamic signal timing to permit WALK phase extensions

This systems-safety approach was also echoed in an innovative signal design launched in 2006 in the UK called Pedestrian User-Friendly Intelligent (PUFFIN) crossings. PUFFIN crossings have the ability – through passive pedestrian detection – to extend the amount of time needed to cross the intersection, such that if a pedestrian is going slower than the assumed pedestrian pace, they will still be served by the signal with an extended WALK phase (Fisher et al., 2010). This could allow a slow-moving senior to receive a time-allowance closer to 2.5 ft/sec without requiring 2.5 ft/sec to be the default basis for signal timing. However, the PUFFIN accommodation capabilities are only as effective as the pedestrian detection system they rely on. PUFFIN signals were limited by errors in the available sensor technology, and further research has investigated supplementing/enhancing the detection zones to optimize the tradeoffs between vehicle delay and pedestrian accommodations (Hassan et al., 2017).

When traffic signals can detect pedestrians as readily as they detect automobiles, a more equitable signal design can be implemented. Fortunately, sensor technology has continued to develop in recent years and the needs of autonomous vehicles has pushed for highly accurate sensing capabilities, which may also prove to further technology that is suitable for infrastructure-based applications such as real-time signal timing adjustments. The following section will outline the differences in sensor technologies.

2.3 DESIRED DATA CHARACTERISTICS OF PEDESTRIAN SENSORS

Dynamic signal timing requires a high degree of functionality from a sensor. The detection process must be permanent (not short term); real time (not requiring post-processing); count sensitive (not just detecting presence); directly detected (not estimated through a model); and suitable for use at intersections (not just a path segment). Although a signal

could operate without storing count data, a countermeasure's safety benefits must be quantified through pedestrian count data (Zegeer et al., 2020). The transportation practice has long desired more complete data of pedestrian activity to meet both of these goals (Figure 2) at signalized intersections. Section 2.4 presents sensing technologies beyond our data interests, but is intended to lend context for understanding the interest in LiDAR for traffic signal operations
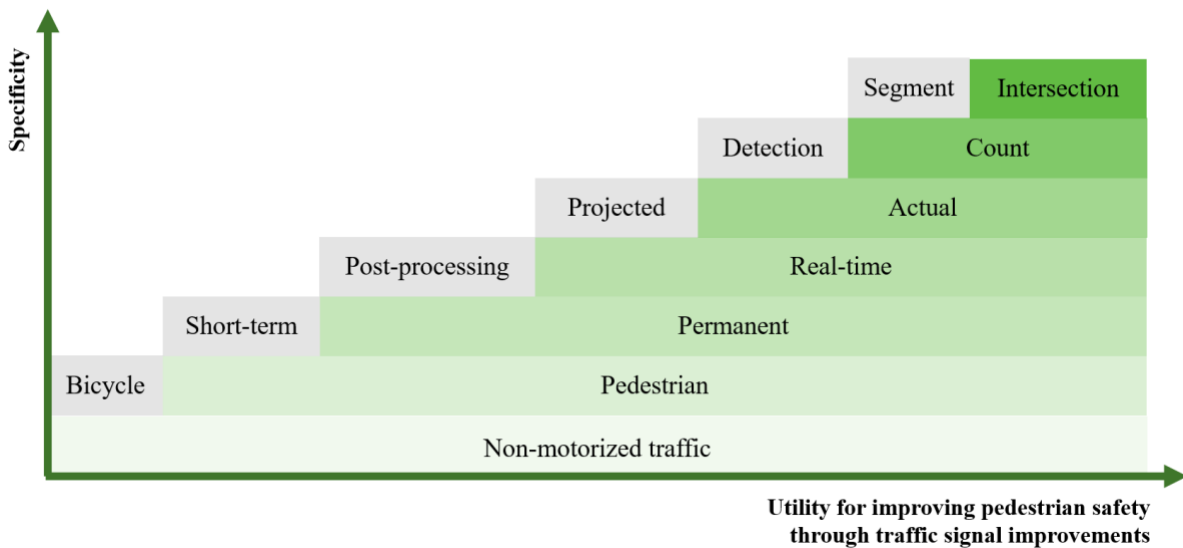
Figure 2.2 Sensor capabilities of interest.

2.4   SENSING MECHANISMS OF DIFFERENT LIGHT WAVES

Sensors vary in the medium by which objects are detected, but several pedestrian sensors rely on electromagnetic waves designed to detect a specific wavelength pertaining to visible light, infrared, microwaves, or radio waves. Electromagnetic sensors can be passive or active. A passive sensor can be compared to the human eyeball: there is a lens to allow light waves to enter and strike a sensing surface that only responds to a specific range of wavelengths. (Correspondingly, the general term "optical cameras" refers to machines that sense the wavelengths of the visible light spectrum.) The passive descriptor refers to the fact that the sensor does not produce the light it senses, it only

has a lens that intercepts ambient waves reflecting in the environment. It does not consume energy to receive the light, only to process it.

Active sensors consume energy to transmit light energy outwards such that some bounces back from the surrounding environment, hits a receiving sensor, and is processed as data. Ranging is the general term used to describe the active sensor mechanism of relating the time between wavelength transmission and reception to a distance between the sensor and its target.

The following descriptions cover various electromagnetic sensors that have been leveraged in pedestrian detection at paved facilities. (Sensors that do not use electromagnetic sensors, such as pressure mats and seismic sensors, are generally limited to trail use (Federal Highway Administration, 2016) and are outside the focus of this project.) Sensor types are presented ordered by the energy intensity of the electromagnetic waves used as their sensing medium. Ultrasonic sensors are not included as they have not attracted much development for future use in smart infrastructure, but extant models operate with many similar active ranging mechanisms, transmitting sound waves instead of electromagnetic waves.

2.4.1 Radar/microwave

Radio detection and ranging (radar) is an active sensor originally explored for military use in the WW II era to detect aircrafts or ships. Since declassification, radar has been leveraged for several civilian uses, especially since radio waves have a wide span of usable wavelengths from 100 meters to 4 millimeters. The longer the wavelength the more material it can pass through, with wavelengths of about 1 meter being used to penetrate the ground for geological surveying. However, longer wavelengths produce lower resolution sensor data (Williams, 2017). For example, radar speed guns used for traffic enforcement can measure vehicle speed using radio wavelengths of about 1 cm. Shorter radio waves are used for higher-resolution applications, such as AV radar sensors emitting waves of about 3-4 mm.

Although an introductory explanation of the electromagnetic spectrum typically positions radio waves as longer wavelength/lower energy than microwaves, the distinctions between radio and microwaves vary by industry, with radio waves being the broader category, and some regarding microwaves as a higher-energy type of radio wave. For this reason, pedestrian sensors transmitting 13 or 24 GHz frequencies are sometimes called radar and sometimes called microwave sensors.

Radar has been used in advanced driver assistance system (ADAS) features, and were used in some the aforementioned PUFFIN crossings to detect pedestrians moving the crosswalk (Manston, 2011). When necessary, a dual antenna system can provide a curbside detection zone and a crosswalk detection zone. Limitations of radar include susceptibility to error from rainfall, though a 13 GHz radar has improved upon this limitation from earlier 24 GHz models. Radar can be used to detect pedestrians up to 30 meters away, though sensors for commercial application generally specify a range of 18 meters.

A Doppler radar system can only detect moving objects, but not a pedestrian standing still. Due to the motion necessary for Doppler radar, more radar-based pedestrian sensors have been developed for use on automobiles (Heuel and Rohling, 2012; Hyun et al., 2016; Institute of Electrical and Electronics Engineers and IEEE Aerospace and Electronic Systems Society, 2010).

2.4.2 Thermal cameras/passive infrared

Thermal cameras and passive infrared (PIR) sensors both use passive detection of infrared light, which sense a shorter wavelength of 8-14 micrometers. Infrared light is radiated from everything according to its heat energy, also known as a heat signature. The higher energy of infrared light (compared to microwaves) enables further high-resolution imaging.

Both PIR sensors and thermal cameras rely on a temperature sensitive resistor, such that when infrared light passes through the lens and strikes the sensor, its electrical resistance changes. The changes in resistance are measured and translated into temperature readings. Passive infrared sensors are typically installed such that when pedestrians pass through a detection zone, their heat signature is counted (Yang et al., 2011). A basic example are the automated doors at public buildings, which use infrared sensing to detect when to open. Early models of pedestrian PIR sensors had narrow detection zones, and thus were sensitive to occlusions – when one pedestrian is eclipsed by another pedestrian walking closer to the infrared bean. This is more likely to occur in crowded conditions, but improvements in data processing have allowed even slightly staggered pedestrians to be distinguished. PIR sensors can also suffer missed detections when the detection zone is narrow. Methods of correcting systematic undercounting have been included in detection literature (Yang et al., 2011). In mixed-traffic areas, bicyclists and pedestrians cannot be distinguished unless an induction loop is installed in the bicyclist's expected path and the pedestrian count extracted from the overall count (Kothuri et al., 2017).

A thermal camera operates with the same detection mechanism, except a matrix of several small sensors all take heat signature readings and ascribe them to a color to create an image. Most thermal cameras have 160x120 IR-sensitive sensors to create 160x120 pixel images and can take such recordings at nine frames per second. Image recognition technology can then be applied to classify objects such as pedestrians, bicyclists, and vehicles (Larson, 2020).

2.4.3 Active infrared

Active infrared sensors emit a beam of infrared light to a receiver located across a pedestrian path. When a pedestrian passes through the path, the beam is blocked and a pedestrian count is recorded. Active infrared counters cannot distinguish between pedestrians and bicyclists, and generally have a narrow detection range. Therefore, they are generally used for pedestrian-only trails, where the pedestrian path is constrained and classification is not necessary (Kothuri et al., 2017; Ozbay et al., 2010).

Active infrared sensors are a good low-cost technology to increase ped counts on trails, but are not being explored for use at intersections or in high-traffic areas.

2.4.4 LiDAR

Light detection and ranging (LiDAR) sensors are active sensors, with applications for industries as diverse as forestry, surveying, altimetry and varying scales of detection and image resolution. For transportation purposes, LiDAR has used been used for supporting automated driver assistance systems (ADAS) such as detecting objects (Garcia et al., 2009) and other collision warning systems. LiDAR has been an interest of AV operations because it is generally held that an instantaneous, localized 3D map of the environment around an AV is necessary for its satisfactory operation (Thakur, 2016).

2.4.4.1 3D LiDAR

3D LiDAR sensors emit rapid pulses of narrow light beams in an ordered raster pattern; when the beams reflect off objects in the surrounding environment, distances can be calculated and stored in a point cloud. Precursors of modern LiDAR were called "laser scanners"; the lasers scan the environment much like a reader scans text. Precise micro electrical mechanical systems (MEMS) use mirrors to control the scanning motions to enable higher-frequency scans and higher-resolution imaging (Kim and Park, 2016). These systems are mechanically complex and expose the sensors to operational vulnerabilities through both mechanical and software errors. These sensors also tend to be expensive and energy intensive. Most 3D LiDAR systems for transportation applications use wavelengths of 1,550 nanometers – because it is possible for the laser to land on an eyeball – and 1,550 nm lasers are considered "eye-safe."

2.4.4.2   2D LiDAR

2D LiDAR emits a wide, diffuse laser that is comparable to the flashing of a camera –
hence, they are often called "flashing LiDAR." Because the light beam is diffused a 905
nm wavelength is safe to human eyes, but also a short enough wavelength to support
high-resolution sensing (Turley, 2018). Because the flashing blankets the area detection
field, the complex mechanical needs laser scanning is eliminated. This is a particularly
promising differentiator for traffic-sensing applications, as the minimization of mechanical
reliance allows the overall sensor size to be smaller and the manufacturing processes to
be less expensive (Turley, 2018). Because a diffuse laser will receive an attenuated
degree of reflected light, flashing LiDAR is not suitable for long-range detection. However,
its range is suitable for detecting pedestrians from a fixed position on a traffic signal. Even
though the ranging capabilities are stronger for 3D LiDAR, 2D LiDAR can support
distance measurements by measuring the qualities of the returned light.

2.4.5 Optical cameras

Digital optical cameras have had a high degree of development due to their ability to
reproduce images like that of human eyesight. Optical cameras are passive; ambient light
in the electromagnetic spectrum enters the lens, passes through filters, and hits several
small units of semiconductor material called photosensors. Light hitting the photosensors
makes small changes in its electrical current, which are captured as image data.
Most optical cameras are RBG cameras and the filters between the lens and photosensor
separate the light into red, green, and blue layers for image processing. However, other
kinds of optical cameras exist, which use different kinds of filters to capture different image
data. Many kinds of optical cameras are being evaluated for use in image recognition and
machine learning (Kilambi et al., 2008; Li et al., 2012).

Optical cameras have the potential to produce the highest-resolution 2D images, but their
detection is severely limited by unfavorable lighting conditions such as darkness or high-
intensity glare (Larson, 2020). Shadows can also degrade performance. Moreover, optical
cameras may produce extra concerns over privacy and personally identifiable information
and thus their data must be managed according to high privacy protections. For these

challenges, LiDAR may offer the best sensing for pedestrians given its balance between the tradeoffs in resolution, the limits of suitable wavelengths, and reliability in wide-ranging lighting conditions.

2.5   SUMMARY

The literature review lays an appropriate context to explain why a shift from fixed assumptions in signal timing to dynamic signal operations can enhance the way pedestrians are accommodated at intersections. Dynamic signal capabilities would not only enhance accommodations (i.e., WALK phase extensions) for those with slower mobility, but also allow for the higher walk speed assumptions to be used as defaults such that vehicle delay is minimized. The success of dynamic signal operations depends heavily on the capability of the sensors. There have been many sensor developments that utilized electromagnetic waves as their sensing medium, and the type of wavelength used affects the maximum sensing resolution. LiDAR has a short enough wavelength to support high-resolution sensing and, as an active sensor, it is not as limited by favorable ambient light environments as optical cameras are. 2D flashing LiDAR has less sophisticated mechanical requirements than 3D LiDAR, which can eliminate potential for error as well as permit for smaller sensors.

3.0 DEVELOPING A TRACKING-BASED DYNAMIC FLASHING YELLOW ARROW (D-FYA) STRATEGY FOR PERMISSIVE LEFT-TURN VEHICLES TO IMPROVE PEDESTRIAN SAFETY AT INTERSECTIONS

The surface transportation system is experiencing rapid changes today. Not only is travel demand increasing, but the travel modes are also diversified. People have more choices for travel other than traditional vehicles, from self-driving cars to e-scooters. There are many initiatives toward smart infrastructure and intelligent vehicles at federal, state, and municipal levels to accommodate these new trends. While these efforts are modernizing the transportation system, issues of "equitable safety" are surfacing. According to the National Highway Traffic Safety Administration (NSHTA) report, pedestrian fatalities have increased by 44% from 2010 to 2019. In 2019, 6,590 pedestrians died of traffic crashes, the highest in 30 years (NHTSA, 2020). Unfortunately, these figures suggest that walking or biking on the street is less safe today. While most of our efforts are devoted to improving mobility and safety for vehicles, the safety for pedestrians on roads is left far behind. Choosing walking or cycling over vehicles is not just a matter of choice but a matter of complex social-economic standings. Many underserved and low-income residents have to walk or bike to get to and from their destinations. Technologies should not only serve those who can afford them but also those who need them. Smart transportation is smart only if it provides equitable safety for all road users. In particular, the vulnerable pedestrians should be paid the most attention to. There are many aspects for pedestrian safety improvement from the perspective of technologies. We think the efforts can be categorized into four levels, as shown in Fig. 3.1.
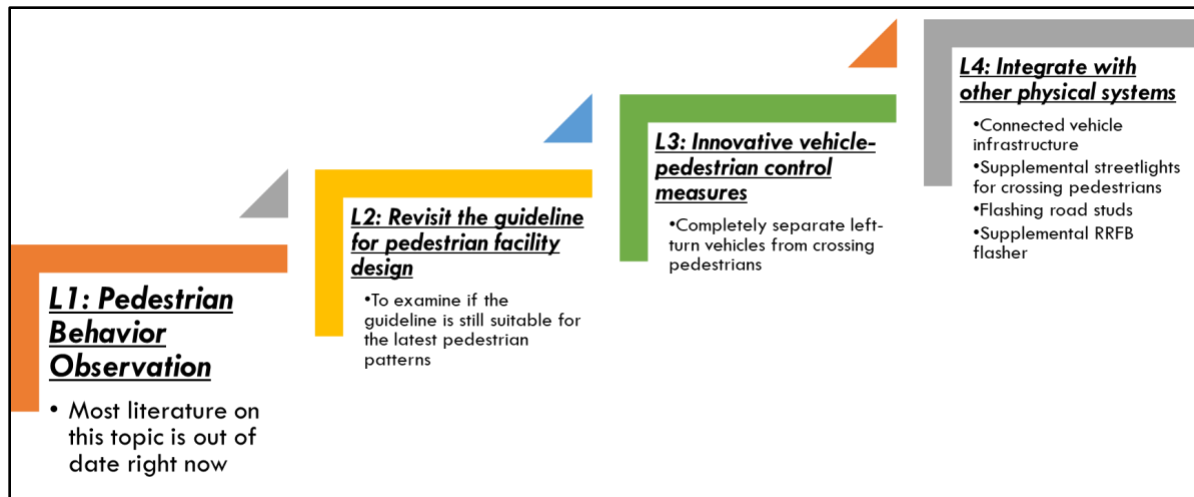
Figure 3.1 Four levels of pedestrian safety improvement.

Level 1: Observe pedestrian behaviors: Pedestrian data are mostly composed of counts today, which are also very limited. While the pedestrian counts reflect the need for pedestrian facilities, they do not necessarily provide observations to determine pedestrian safety. As such, it is necessary to collect pedestrian behavioral data for better-informed decision making toward pedestrian safety improvement.

Level 2: Revisit the design guideline for pedestrian facility design. With more pedestrian behavioral data, it becomes possible to inspect the effectiveness of existing pedestrian facilities and validate the current design guidelines. Level 2 measures are primarily aimed at planning.

Level 3: Novel control measures to improve pedestrian safety: this level involves real-time pedestrian behavioral data collection and real-time pedestrian protection, such as reducing pedestrian conflicts with vehicles. Level 3 measures are primarily aimed at operations. The proposed D-FYA system belongs to this level.

Level 4: Integrate with other physical systems. At this level, multiple physical systems will be integrated to further protect pedestrians. For instance, the D-FYA system can be coupled with a lighting system to provide supplemental lights for crossing pedestrians at night. Level-4 solutions are rare today, but those novel solutions may be highly effective at protecting pedestrians.

Here, we propose a dynamic flashing yellow arrow (D-FYA) mechanism based on a state-of-the-art LiDAR tracking system to fully protect concurrent crossing pedestrians. This system fits into the Level-3 pedestrian protection activities defined above. The major benefit of this new D-FYA method is to completely separate the concurrent crossing pedestrians from permissive left-turn vehicles while using all safe permissive left-turn capacities. This feature is especially beneficial when a phase duration is much longer than the required pedestrian crossing time.

3.1 DYNAMIC FLASHING YELLOW ARROW STRATEGY BASED ON LIDAR-BASED PEDESTRIAN TRACKING TECHNOLOGY

Flashing yellow arrow (FYA) has been widely adopted for permissive left-turn movements after the related research concluded that the FYA would improve traffic safety (Noyce et al., 2014). However, the current FYA mechanism does not separate permissive left-turn vehicles from concurrent crossing pedestrians. As a result, pedestrian crashes reportedly increased at certain locations after the implementation of FYA. To address this issue, agencies either turn the FYA off or adopt a special feature in some brands of traffic signal controllers, referred to as "minus pedestrian." The concept is temporarily suppressing the FYA for a cycle if the corresponding pedestrian phase is called. Fig. 3.2 shows the concepts of FYA and the "minus pedestrian."
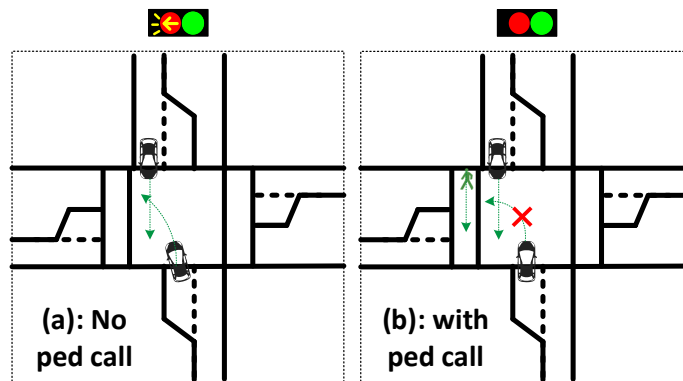
Figure 3.2 Demonstrations of FYA and "minus pedestrian."

Although the "minus pedestrian" feature separates left-turn vehicles from concurrent crossing pedestrians, it also eliminates all the permissive left-turn capability for that cycle. This mechanism often creates excessive left-turn queues during peak hours when both pedestrian volumes and left-turn vehicle volumes are high. We design a new dynamic

FYA or D-FYA based on a LiDAR-based pedestrian tracking system to address this issue. As shown in Figure 3.3, concurrent crossing pedestrians have a conflict with left-turn vehicles only when they are within the so-called "hazard zone."

"Three-zone" pedestrian tracking with LiDAR sensors: In reality, there may be situations where pedestrians may push the pedestrian button and then choose to cross or "jaywalk" before the WALK sign starts. As a result, neither a pedestrian phase nor FYA suppression is needed for that cycle. The main objective of the D-FYA is to protect pedestrians who comply with the traffic signal indications. To address these issues, we design a "three-zone" method to filter and only track those legitimate crossing pedestrians. As shown in Fig. 3.3., a pedestrian needs to enter the wait zone first and push the pedestrian button to be considered legitimate. The waiting zones (Zone 1) of each pedestrian phase are defined as "far-end" (Zone 1) and "near-end," according to their relative locations to the left-turn vehicles. During WALK, if a pedestrian is in Zone 1 and/or 1' enters the boundary zones (Zones 2 and 3), then this pedestrian is considered a legitimate pedestrian. If the same pedestrian reaches the other end, then this pedestrian crossing is considered finished. If the pedestrian button is pushed but no legitimate pedestrians enter the intersection, the pedestrian request is then considered void and ignored. The three-zone method will filter out those "jaywalking" pedestrians.
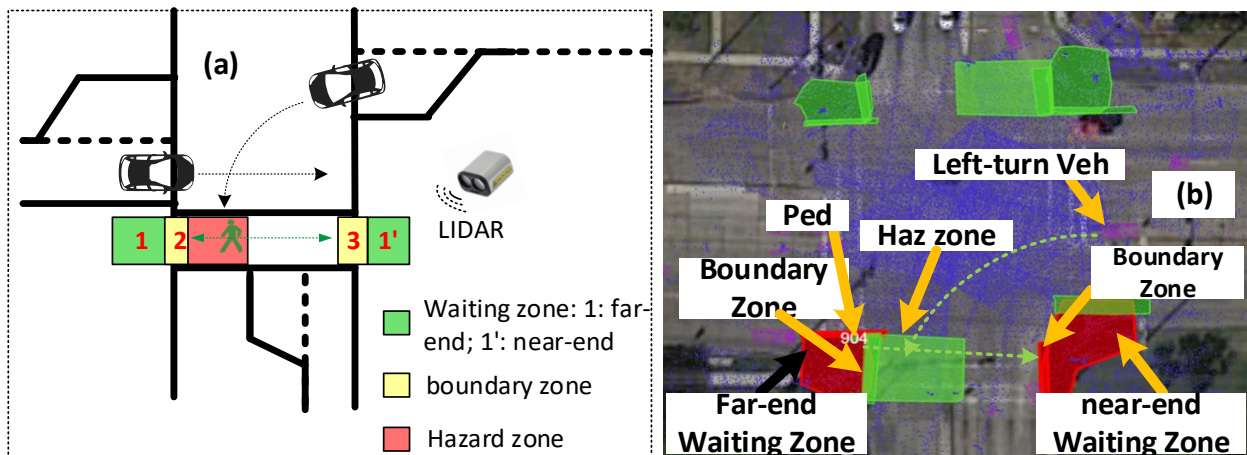
Figure 3.3 Three-zone pedestrian detection method at intersections: a: demonstration, b: zone settings in the field in reference to WB left-turn vehicles (City of Irving, TX).

Dynamic Flashing Yellow Arrow (D-FYA) based on pedestrian tracking: The D-FYA algorithm is elaborated as follows:

When a traffic signal green phase starts: Reset all the FYAs as programmed initially.

When this signal phase enters yellow and all-red: The proposed D-FYA algorithm will check the following items in sequence:

STEP 1: Check if this phase has a concurrent pedestrian phase. If yes, go to Step 2. If no, STOP.

STEP 2: Check if the pedestrian button is pushed. If yes, go to Step 3. If no, STOP.

STEP 3: Examine the presence of pedestrians in far-end and near-end waiting zones. There are two scenarios:

(i) No pedestrians are detected at either waiting zones, the D-FYA algorithm will keep the original FYA settings. Then go to STEP 4.

(ii) Pedestrians are detected at one or two waiting zones, then the D-FYA algorithm will suspend the programmed FYA temporarily. Then go to STEP 4.

When green or WALK starts, the D-FYA algorithm will check STEP 4 through 6 to make the final decision on FYA for this cycle.

STEP 4: At this step, there are four possibilities for pedestrians to enter the intersection from two sides of the waiting zones.

(i) During the WALK time, if pedestrians in the far-end waiting zone (e.g., Zone 1 in Fig.3.3) enter the intersection (e.g., Zone 2 in Fig. 3.3) but no pedestrians in the near-end waiting zone (e.g., Zone 1' in Fig. 3.3) enter (e.g., Zone 3 in Fig. 3.3). The FYA is suspended until all pedestrians have left the "hazard zone" (See Fig. 3.3). Then the FYA is reactivated until the current phase ends.

(ii) During the WALK time, if pedestrians in the near-end waiting zone enter the intersection while no pedestrians in the far-end waiting zone enter, then the FYA is suspended until all near-end pedestrians reach the other side of the intersection (e.g., enter the boundary zone on the other side). Then the FYA is reactivated until the current phase ends.

(iii) During the WALK time, if pedestrians enter the intersection from both sides, the FYA is suspended until all pedestrians reach the other side.

(iv) During the WALK time, if no pedestrians enter from either side, the FYA is activated until the current phase ends.

Step 4 is the final step of this algorithm for each phase.

Discussion:

1. Note that the decisions on FYA at Step 3 are temporary because a detected person in the waiting zones does not mean they intend to cross, or a pedestrian may mistakenly push a pedestrian button. The final decision of keeping or suspending an FYA will be determined after the green/WALK display indication starts.

2. Note that activating FYA or not is made once and only once with each cycle to avoid confusing drivers and pedestrians.

3. If a pedestrian "jaywalks" and gets out of the boundary zone when reaching the intersection's other side, LiDAR sensors will lose tracking it. The missing pedestrian will be allocated with a longest walk time beyond which this person is considered to have crossed.

4. The proposed D-FYA is particularly effective when the opposing green is much longer than the needed pedestrian crossing time. Once all pedestrians are cleared, the FYA is reactivated and can provide a significant permissive capacity for left-turn vehicles. By contrast, the current "minus pedestrian" mechanism will unconditionally suppress the FYA all through the cycle even if no pedestrians cross after the push button is pressed or all pedestrians have crossed the intersection during a short period.

3.2   ANALYSIS OF PERMISSIVE LEFT-TURN CAPACITY UNDER D-FYA

In this section, we analyze the changes to the permissive left capacity with the D-FYA as opposed to that with the PPLT under different scenarios. A traffic scenario in this context is composed of the duration of D-FYA, opposing through traffic volumes and the number of lanes, and the corresponding pedestrian volume. After the protected left-turn phase is over, the FYA will start together with the green for the opposing through traffic. The left-turn vehicles will begin to seek acceptable gaps to maneuver. While the queue of opposing traffic is being discharged, the left-turn vehicles cannot find the gaps due to the small headways. After the queuing vehicles are cleared, the left-turn vehicles will be able

to find acceptable gaps to cross. If the permissive left-turn strategy is D-FYA, then the flashing yellow arrow may start on time, be delayed, or even canceled, depending on the presence of pedestrians. It can be formulated as follows. Table 3.1 shows the notation for the formulation.

Table 3.1: Notation for analysis of permissive left-turn capacity under D-FYA

Notations for Analysis of permissive left-turn capacity under D-FYA	
C	Cycle length (sec)
G	Green duration of opposing through traffic
s	Saturation rate (vehicle per hour per lane)
q	Volume of opposing through traffic (veh per hour per lane)
p	Volume of concurrent crossing pedestrians (ped per hour)
T	Time window for permissive left turn (sec)
T'	Time window for permissive left turn under D-FYA (sec)
t_c	Queue clearing time (sec)
h	Headway (sec)
h_a	Acceptable gap for left turning (sec)
cap_{permLT}	Capacity during the permissive protected left turn (veh per hour per lane)
$\overline{cap_{permLT}}$	Capacity during FYA (veh per hour per lane)

As shown in Fig. 3.4, t_c is the time for clearing the queue of opposing through traffic and it can be calculated as:

Total arrivals during red and queue clearing time: $q \times (C - G + t_c)$

Total departures during the queue clearing time: $s \times t_c$

Then total arrivals are equal to total departures when the queue is cleared.

$$q \times (C - G + t_c) = s \times t_c \tag{1}$$

Therefore,

$$t_c = \frac{(C-G)}{\left(\frac{s}{q}-1\right)} \tag{2}$$

During t_c, left-turn vehicles cannot find acceptable gaps. The permissive time window for the left-turn vehicles with a cycle is:

$$T = G - t_c = G - \frac{(C-G)}{\left(\frac{s}{q}-1\right)} = \frac{(sG-qC)}{(s-q)} \tag{3}$$
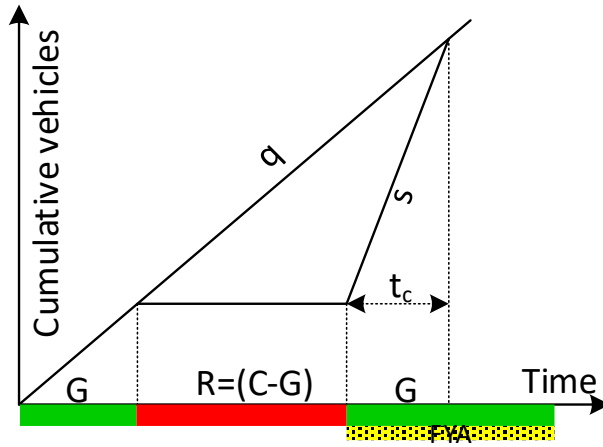
Figure 3.4 Queue clearing time calculation with the cumulative counting curves.

Assuming that new opposing through vehicles arrive randomly, then the headway between arrivals can be approximated by an exponential distribution. The CDF function of the headway h is

$$F_{(h,q)} = \begin{cases} 1 - e^{-qh} & h \geq 0 \\ 0 & h < 0 \end{cases} \quad \text{(Multiple lanes)} \tag{4}$$

$$F_{(h,q)} = \begin{cases} 1 - e^{-qh} & h \geq h_{safe} \\ 0 & h < h_{safe} \end{cases} \quad \text{(Single lane)} \tag{4-a}$$

From (4) and (4-a), after the queue is cleared, the mean headway in seconds will be $\left(\frac{3600}{q}\right)$ seconds and the expected number of gaps of opposing through traffic during the permissive left-turn time window will be $\frac{T}{\left(\frac{3600}{q}\right)}$. We can also estimate that the probability that headway is equal to or greater than the acceptable gap is:

$$F_h\{h > h_a\} = 1 - (1 - e^{-qh_a}) = e^{-qh_a} \tag{5}$$

So, the maximal left-turn capacity during the permissive time window will be

$$cap_{permLT} = \frac{T}{\left(\frac{3600}{q}\right)} \times e^{-qh_a} = \frac{(sG-qC)}{(s-q)} \times q \times e^{-qh_a} \tag{6}$$

The average pedestrian arrivals per cycle n_p can be calculated as

$$n_p = \frac{p}{\left(\frac{3600}{C}\right)} \tag{7}$$

27

When pedestrians are only on the near side or on both sides (See Fig. 3.4), then they will use all the walk and pedestrian clearance time to cross the intersection. During that period, the D-FYA will indicate a red arrow for left-turn vehicles. After the pedestrian clearance timer expires, FYA will be displayed. As such, the remaining permissive time window T' will be

$$T' = T - t_{WALK} - t_{PC} = \frac{(sG-qC)}{(s-q)} - t_{WALK} - t_{PC} \tag{8}$$

And the permissive left-turn capacity is

$$\frac{T'}{\left(\frac{1}{q}\right)} \times (1 - e^{-qh_a}) = \left(\frac{(sG-qC)}{(s-q)} - t_{WALK} - t_{PC}\right) \times q \times e^{-qh_a} \tag{9}$$

When pedestrians are only on the far side, they will take about 50% of pedestrian clearance time to cross the "hazard zone." Then the D-FYA will start the flashing yellow arrow for left-turn vehicles and so the permissive left-turn capacity in this case is

$$\left(\frac{(sG-qC)}{(s-q)} - - t_{WALK} - \frac{t_{PC}}{2}\right) \times q \times e^{-qh_a} \tag{10}$$

If $n_p \leq 1$, then the presence probability of one crossing pedestrian with each cycle will be n_p and the pedestrian can appear either on the near side or far side with equal (50%) probabilities (See Fig. 3.4). The expected permissive left-turn capacity under D-FYA can be estimated as

$$\overline{cap_{permLT}} = \frac{\left(\left(\left(\frac{(sG-qC)}{(s-q)} - - t_{WALK} - t_{PC}\right) \times q \times e^{-qh_a}\right) + \left(\left(\frac{(sG-qC)}{(s-q)} - - t_{WALK} - \frac{t_{PC}}{2}\right) \times q \times e^{-qh_a}\right)\right)}{2} \tag{11}$$

If $n_p > 1$, then we can assume there is more than one pedestrian every cycle and they can all be on the near side, on the far side, or both sides with equal (33%) probability. The expected permissive left-turn capacity of the D-FYA can be estimated as

$$\overline{cap_{permLT}} = \frac{\left(2 \times \left(\left(\frac{(sG-qC)}{(s-q)} - - t_{WALK} - t_{PC}\right) \times q \times e^{-qh_a}\right) + \left(\left(\frac{(sG-qC)}{(s-q)} - - t_{WALK} - \frac{t_{PC}}{2}\right) \times q \times e^{-qh_a}\right)\right)}{3} \tag{12}$$

Table 3.2 Traffic settings for the permissive left-turn capacity calculation

	Permissive LT			D-FYA (np<1)			D-FYA (np>=1)		
Cycle length	110	110	110	110	110	110	110	110	110
opposing through green (s)	34	40	46	42	48	54	42	48	54

saturation rate (vphpl)	1500	1500	1500	1500	1500	1500	1500	1500	1500
the volume of opposing through traffic (veh per hour p)	400	500	600	400	500	600	400	500	600
Crossing ped volumes (ped per hour)	100	200	300	100	200	300	100	200	300
Through queue clearing time	3	3	3	3	3	3	3	3	3
time window for permissive LT	14	30	12	14	30	12	14	30	12
Acceptable gaps for permissive LT	8	8	8	8	8	8	8	8	8
pedestrian clearance time (sec)	5	5	5	5	5	5	5	5	5
pedestrians walk time (sec)	10	10	10	10	10	10	10	10	10

Table 3.3 shows the sensitivity results of capacity under different conditions.

Table 3.3: The sensitivity results of capacity under different conditions

Single Lane			
Oppose Th Volume (v/h/l)	Perm LT Cap in PPLT	D-FYA (np<1)	D-FYA (np>=1)
400	1632	903	797
500	1434	717	598
600	1027	642	513
Multiple Lane			
Oppose Th Volume (v/h/l)	Cap of Perm LLT	D-FYA (np<1)	D-FYA (np>=1)
400	1046	579	511
500	823	535	466
600	527	329	264

Fig. 3.5 shows the permissive left-turn capacity under different capacities.
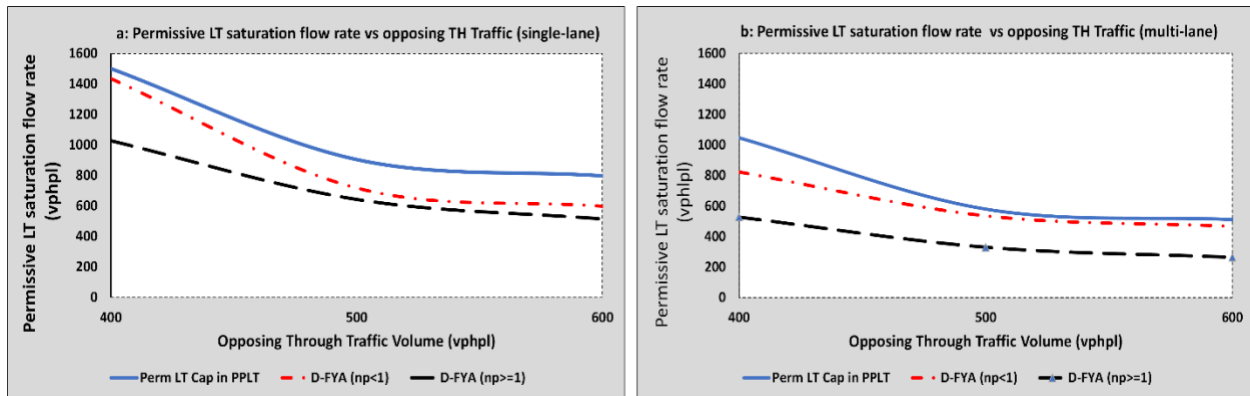
Figure 3.5 The sensitivity of capacity under different conditions: (a) single lane (b) multiple lanes.

Discussion:

1. From Eq. (6), if the opposing through traffic volume q is high, the permissive left-turn capacity will be close to zero. In that case, the traffic signal timing should only use a protected left-turn strategy to discharge the left-turn vehicles.

2. From Eq. (11) and Eq. (12), if the mainline green is much longer than the walk and pedestrian clearance time or even almost equal to the cycle length, then the D-FYA will reserve significant permissive left-turn capacities while separating the pedestrians from left-turn vehicles. By contrast, the PPLT with minus pedestrian phase will not reserve any permissive left-turn capability when pedestrians arrive with every cycle.

3. The above analysis is limited to isolated intersections because it assumes random arrivals of opposing through traffic after the queue is cleared. If an intersection is on coordination, then exponentially distributed headway for new arriving vehicles may be no longer valid because upstream vehicles will arrive in platoons. The analysis of acceptable gaps for coordinated intersections must be empirically performed.

3.3 CASE STUDY I: EVALUATION OF D-FYA'S PERFORMANCE USING THE "EMULATION-IN-THE-FIELD" TRAFFIC SIGNAL SIMULATION FRAMEWORK

In this experiment, we evaluated the performance of the proposed D-FYA algorithm in the field by verifying its real-time decisions according to the observed pedestrian behaviors

in the field. The experiment design is referred to as the "emulation-in-the-field" framework. It means all the traffic signal inputs and pedestrian behaviors are instantaneously collected in the real world to drive the D-FYA decision makings, whereas the D-FYA decisions are not implemented but reported to the observers for verification. The purpose of this experiment is to evaluate the algorithm's reliability and accuracy in the field. The selected intersection is Cooper Street at the UTA Boulevard, a major intersection connecting two urban campuses of the University of Texas at Arlington. The daily pedestrians crossing Cooper Street (mainline) range from 1,000 to 1,500 in a school day. The phasing sequence and pedestrian tracking zones are shown in Fig. 3.6. There are four flashing yellow arrows on all four approaches.

Whenever a phase starts, the D-FYA algorithm will run and report its findings (e.g., the presence of waiting pedestrians) and decisions (e.g., suppressing or activating an FYA) on the console screen. At the same time, a researcher verified the reported decisions according to their observations in the field based on the expected decisions according to the algorithm. The observation was carried out over 100 signal cycles with pedestrian crossings. Table 3.4 demonstrates how the D-FYA decisions were recorded and verified, using five cycles as an example.
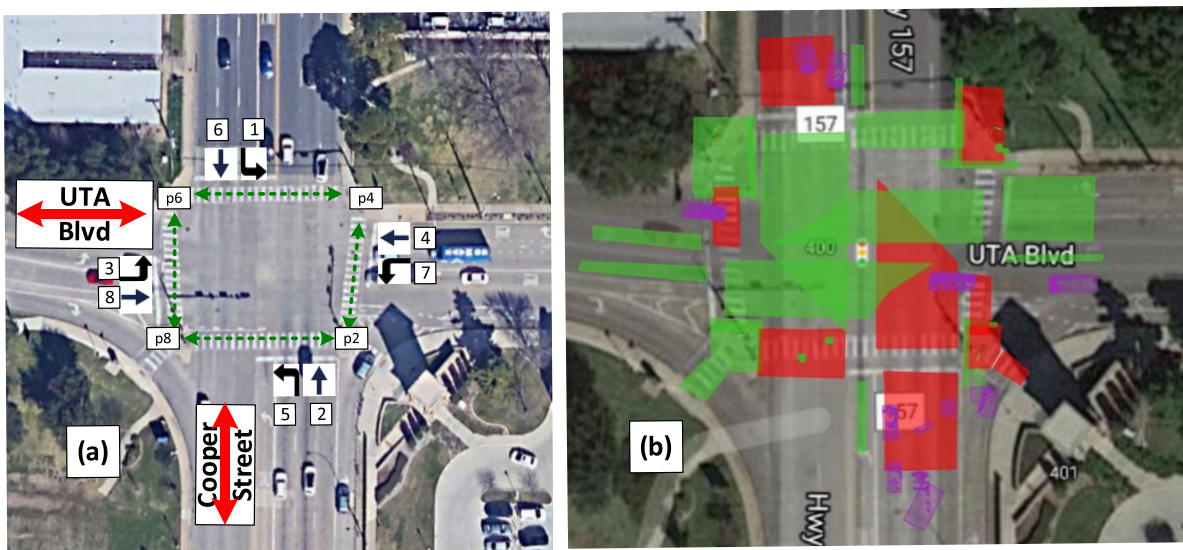
Figure 3.6 Phasing sequence (Fig. 3.6-a) and pedestrian sensing zone layout (Fig.3.6-b) at Cooper Street and UTA Boulevard, Arlington, TX.

Table 3.4 Records of emulation-in-the-field to verify the D-FYA strategy

Signal Cycle	Corresponding signal phases	near-end ped presence	far-end ped presence	Both ends ped presence	No ped presence	FYA started as scheduled	FYA delayed	FYA cancelled	Comment
1	8	1	0	0	0	0	0	1	1*
2	4	1	0	0	0	0	1	0	1*
3	4	0	0	0	1	1	0	0	2*
4	4	1	0	0	0	0	1	0	1*
5	4	0	1	0	0	0	1	0	1*

Note: 1*: verified by the researcher in the field; 2* verified that the push button was pressed but the pedestrian chose not to wait (either jaywalked or walked away)

The case study was conducted for 100 cycles in the field. There were 70 cycles where at least one pedestrian phase was called. Among those 70 cycles, 25 cycles only had near-end pedestrians, 25 cases with far-end pedestrians, nine cases with pedestrians on both sides, and 11 cases with pedestrians walking away before WALK. Comparing what the D-FYA was reported on the screen and what we observed in the field, we concluded that the D-FYA algorithm could make correct decisions in 93 cycles out of 100 cycles. Table 4 summarizes the D-FYA's performance under various scenarios.

Table 3.5: Performance summary of D-FYA algorithm under different scenarios

Cycles with no ped calls	Cycles only with near-end peds	Cycles only with far-end peds	Cycles with both-end peds	Cycles with ped calls but no ped presence	The accuracy rate of the D-FYA algorithm
30	25	25	9	11	93%

After finishing the experiment in the field, we further analyzed the recorded video and identified the possible reasons for incorrect D-FYA decisions. In those failed cases, the pedestrians either leaned on the traffic light poles or multiple pedestrians stood too close for the LiDAR tracking algorithm to separate them effectively. This accuracy rate should further increase with improvements to the LiDAR tracking.

3.4 CASE STUDY II: MOBILITY EVALUATION OF THE D-FYA STRATEGY USING THE "CABINET-IN-THE-LOOP" TRAFFIC SIGNAL SIMULATION PLATFORM

In the second case study, we evaluate the mobility performance of the D-FYA as opposed to the other two common permissive left-turn strategies: (I) protected + permissive left turn (PPLT); and (II) protected + permissive + minus-ped-phase. The first strategy is to

show the left-turn vehicles with a green arrow followed by a flashing yellow arrow, whereas the second strategy is to show the left-turn vehicles with a green arrow first and then examine if a pedestrian call is placed. If so, then a red arrow is displayed until the end of opposing green. Otherwise, the flashing yellow arrow is activated.

The intersection of West Walnut Hill Lane at North Belt Line Road in Irving, TX, was selected to develop a simulation model. Fig. 3.7 shows the movements and phasing sequence.
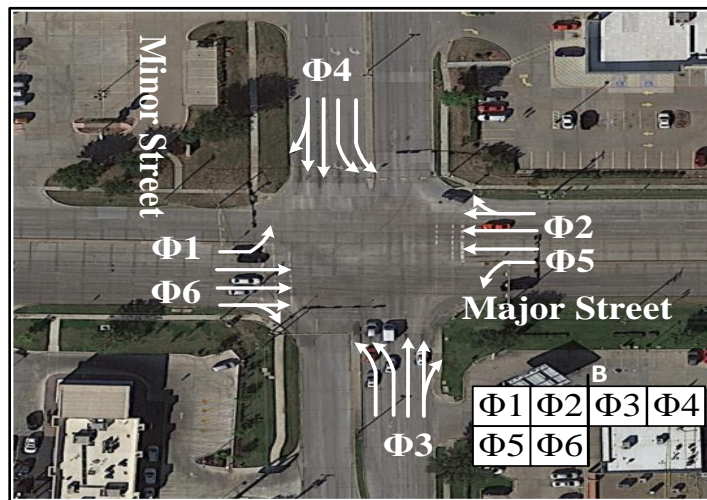
Figure 3.7 Layout of intersection for the second case study.

Cabinet-in-the-loop traffic signal simulation platform: The "minus-ped-phase" feature was not available in traffic signal controllers until very recently. So, it is not yet supported by any traffic signal simulation engine. To keep a high-fidelity and fair comparison, we developed a cabinet-in-the-loop traffic signal simulation platform for this experiment. As shown in Fig. 3.8, two control units (CU) are coupled with the VISSIM simulation engine. The first CU is a fully scaled traffic signal assembly. Through the input and out serial ports of the assembly, we retrieved the latest traffic signal status in the traffic signal controller, and we then sent it into VISSIM simulation via the provided traffic signal control API. On the other hand, the real-time detector status in the simulation is collected via the signal control API and then sent into traffic signal assembly via its input serial port. The hardware traffic signal controller will decide according to the detector inputs, including the FYA and minus pedestrian phase for the FYA.

A challenge in this experiment is that pedestrian tracking is not straightforward in simulation. To address this issue, we developed a second virtual controller in simulation for the D-FYA strategy. Its logic is to issue a red arrow if there are crossing pedestrians (i.e., the blue detectors are occupied by pedestrians); otherwise, it will issue a green arrow. The virtual controller issues red light only when the pedestrian phase is activated, so when pedestrians (if any) enter the intersection. The simplified D-FYA algorithm will not lose its generality since pedestrians have no random exceptions in a simulation like jaywalking.

As shown in Fig. 3.8, the blue detectors are configured to detect concurrent crossing pedestrians. Two signal heads, controlled by the hardware controller and by the virtual D-FYA controller, respectively, are placed in sequence for the left-turn vehicles. The permissive left-turn vehicles can seek gaps and enter only if neither traffic signal head is red. As an illustration, when the opposing (SB in Fig. 3.8) traffic light turns green with the concurrent pedestrian phase, the hardware traffic signal controller will turn the first signal head to a flashing yellow arrow. In the meanwhile, if the virtual controller detects the presence of crossing pedestrians, it will turn red, preventing vehicles from entering the intersection. If the virtual controller does not detect the pedestrian presence, it will indicate a green arrow. A flashing yellow arrow and a green arrow will allow left-turn vehicles to enter the intersection during the permissive left-turn phase. This configuration can, in essence, start, delay, or cancel a programmed FYA within a cycle.
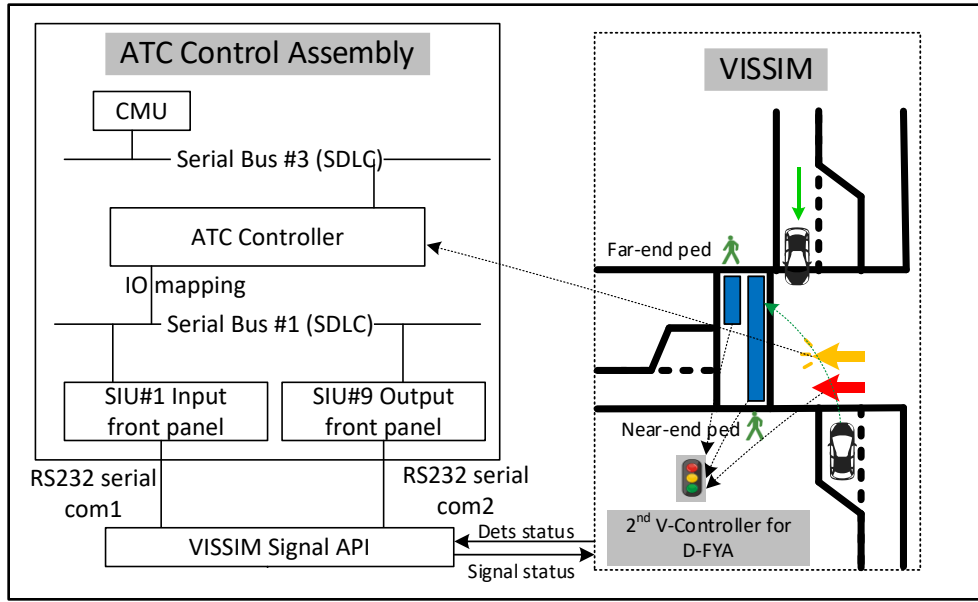
Figure 3.8 The architecture of cabinet-in-the-loop traffic signal simulation for the D-FYA evaluation.

Without loss of generality, the mainline vehicle and concurrent crossing pedestrian volumes are set as low, medium, and high to evaluate the performance of three permissive left-turn strategies (see Table 5). The experiment also excluded the possibility of "starvation" by extending the green on the mainline left-turn lanes to ensure the mainline traffic was not affected by different permissive left-turn strategies.

Table 3.6 Vehicle and pedestrian volumes for different scenarios

Volume	Southbound			Northbound			Westbound			Eastbound			Pedestrian
	L	T	R	L	T	R	L	T	R	L	T	R	
Low	75	200	30	75	200	30	300	500	120	300	500	130	100
Medium	75	200	30	75	200	30	500	500	120	500	500	130	200
High	75	200	30	75	200	30	750	500	120	750	500	130	350

Nine simulation scenarios are generated with the combination of available vehicle and pedestrian volumes. They are referred to as:

1. LVLP: low vehicle volumes and low pedestrian volumes.
2. LVMP: low vehicle volumes and medium pedestrian volumes.
3. LVHP: low vehicle volumes and high pedestrian volumes.

4. MVLP: medium vehicle volumes and low pedestrian volumes.
5. MVMP: medium vehicle volumes and medium pedestrian volumes.
6. MVHP: medium vehicle volumes and high pedestrian volumes.
7. HVLP: high vehicle volumes and low pedestrian volumes.
8. HVMP: high vehicle volumes and medium pedestrian volumes.
9. HVHP: high vehicle volumes and high pedestrian volumes.

Fig.3.9 shows the mainline left-turn queue length (in feet) comparison among three permissive left-turn strategies. It reveals that the mobility performance of D-FYA is between the PPLT and "PPLT with Minus-pedestrian-phase" in most cases. In some cases, the D-FYA is much better than the "PPLT+Minus-Ped-phase" (e.g., the MVHP scenarios) in mobility while separating the left-turn vehicles and pedestrians. When the opposing through traffic and pedestrian volumes are both high, all three permissive left-turn strategies will degrade to the protected-only left-turn strategies (e.g., the HVHP scenario) because the left-turn vehicles cannot find the acceptable gaps. A similar pattern also shows in the delay analysis (Fig. 3.10).

Discussion II

From the simulation results, it can be concluded that for both low vehicle and medium traffic conditions, PPLT and D-FYA has better performance over PPLT+Minus-Ped-Phase strategy whereas the D-FYA and PPLT with Minus-Pedestrian-Phase have the same pedestrian protection. However, when both vehicle and pedestrian volumes increase to a high level, all three permissive left-turn strategies show similar delays and queue lengths to the protected-only left-turn strategy. This is because the left-turn vehicles cannot find the acceptable gaps during FYA. It implies that we may need to prohibit any permissive left-turn strategies under certain scenarios.
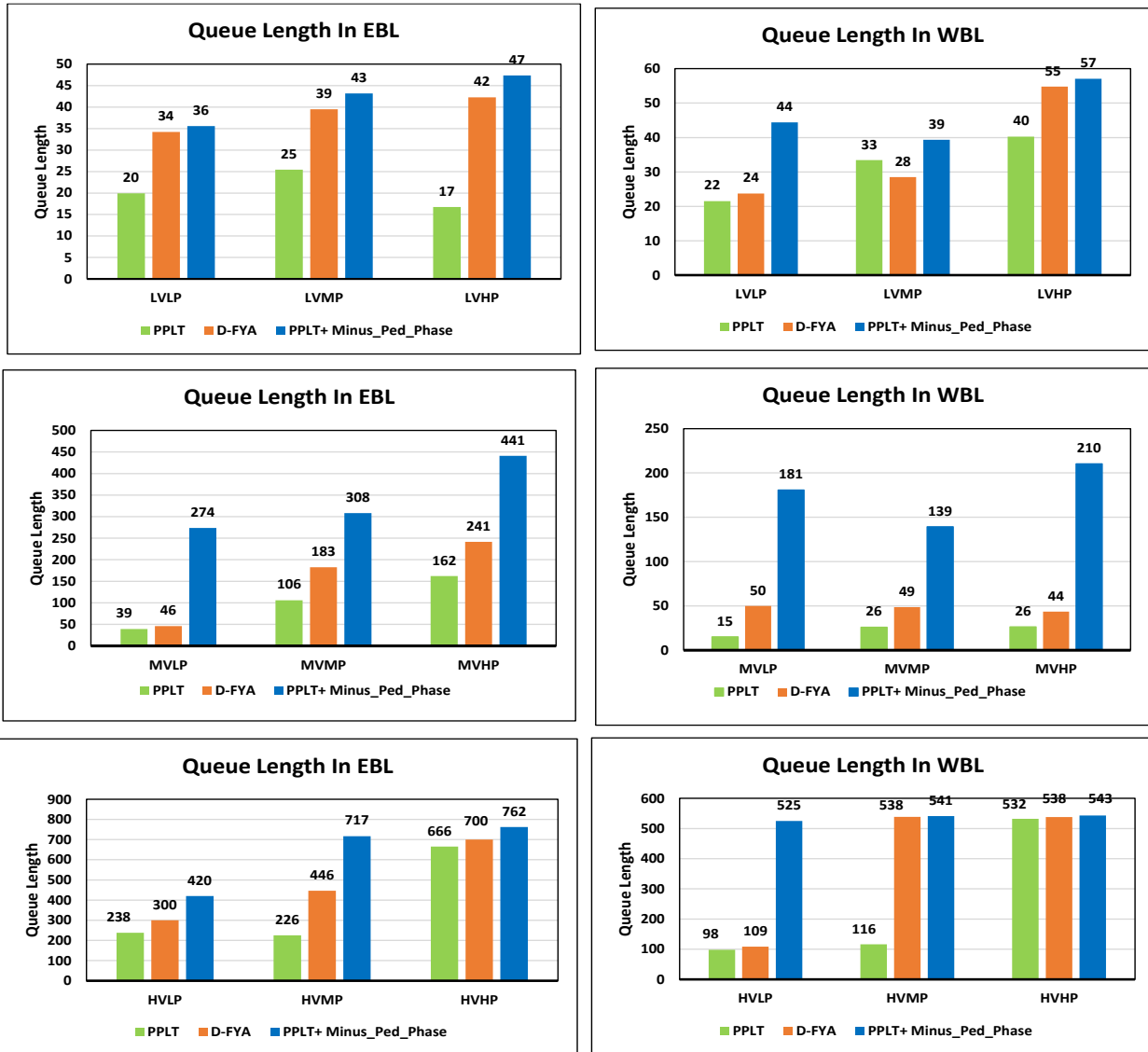
Figure 3.9 The mainline left-turn queue length comparison under various scenarios.
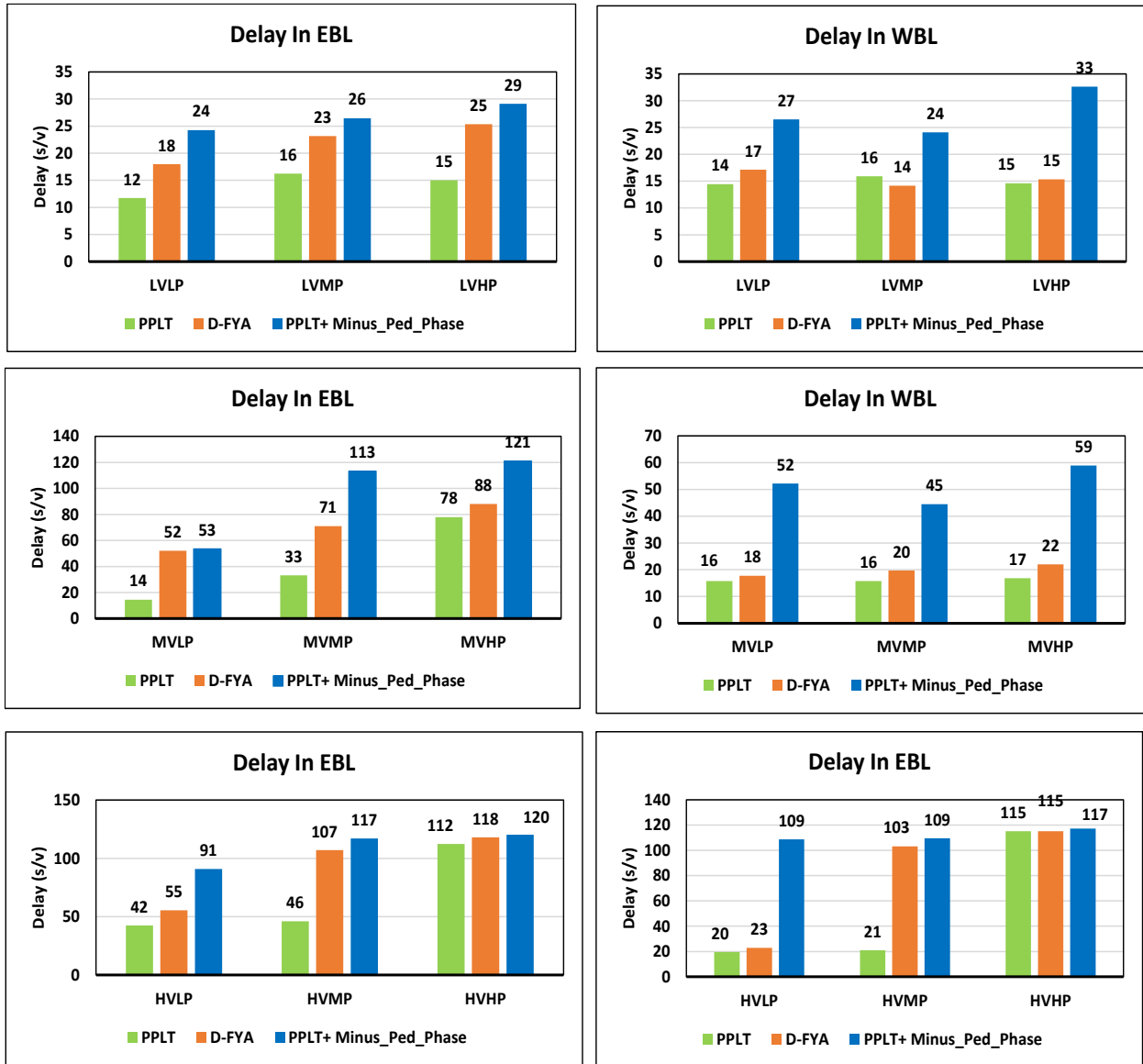
Figure 3.10 The mainline left-turn delay comparison under various scenarios.

3.5 CONCLUSION AND FUTURE WORK

In this study, we develop a novel dynamic flashing yellow arrow (D-FYA) mechanism to leverage the permissive left-turn capacity and crossing pedestrians' safety based on pedestrian tracking technologies. The research outcome is to address the reported potential safety hazards after the flashing yellow arrow (FYA) permissive left-turn strategy is widely deployed. Through a novel "emulation-in-the-field" traffic signal control

framework, we verified the resilience of the proposed D-FYA algorithm to random pedestrian behaviors and mitigations to inaccurate pedestrian detections. In addition, in a controlled simulation environment, we further evaluated all three permissive left-turn strategies: protected-permissive left turn (PPLT), D-FYA, and PPLT with minus-pedestrian-phase. We concluded that the proposed D-FYA-based pedestrian tracking would be more efficient than the PPLT with a minus-pedestrian phase. At the same time, it can effectively solve the issue of pedestrian safety. It was also found that when the opposing through traffic became high, all three permissive left-turn strategies degraded to the protected-only control strategy, leading to high delays and long queues.

In the future, we plan to introduce more features into the D-FYA strategy, considering the concurrent crossing of pedestrians and the opposing through traffic. As revealed in the experiment, it would be better to dynamically cancel and recover the FYA according to the volume of opposing through traffic. It may reduce the possibility of collisions between left-turn vehicles and opposing through vehicles.

4.0 PEDESTRIAN BEHAVIOR STUDY

The literature review lays an appropriate context to explain why a shift from fixed assumptions in signal timing to dynamic signal operations can enhance the way pedestrians are accommodated at intersections. To achieve this objective, a LiDAR device was selected and tested in the field. This chapter provides descriptions of the LiDAR device, site selection, analysis of the data and results.

4.1 SELECTION OF LIDAR DEVICE

The selected LiDAR sensors are directional, and each sensor has a 60-degree field of view. At each intersection for the pilot study, four LiDAR sensors were installed and aligned in such a way that one object (vehicle or pedestrian) can be tracked and carried over from one sensor to the other while keeping the same ID. We adopted a perception software provided by the LiDAR manufacturer. From the preliminary study, it was recognized that the provided perception software might capture false objects under certain conditions (heavy rains, snows, etc.). To mitigate this issue, the project team developed an additional context-aware screening algorithm. For instance, if an "object" was reported to appear in the middle of an intersection for a long time, this object will be ignored because this is unrealistic. With the provided tools, the project team also drew zones within the sensing area and developed a computer program to retrieve zone status and synchronize with signal controller status for the proposed research. Fig. 4.1 demonstrates the system architecture.
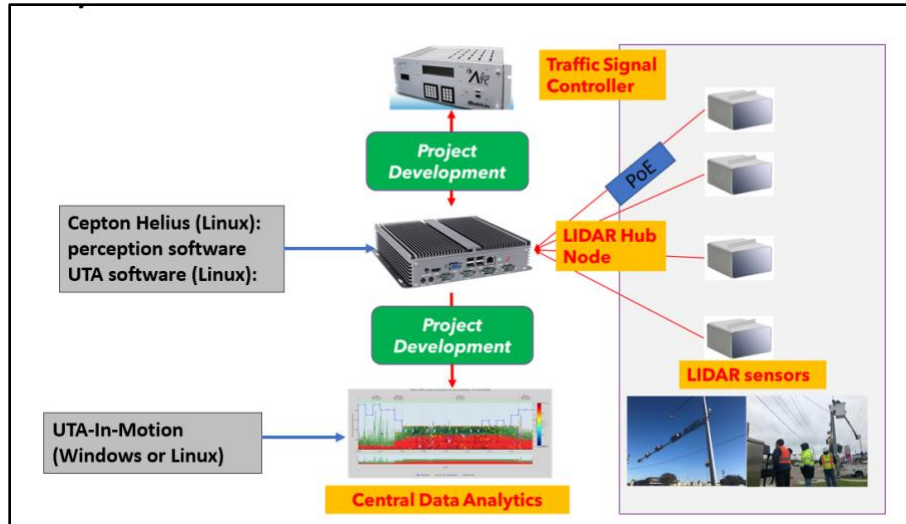
Figure 4.1 System architecture of the pedestrian information system.

4.2 ALGORITHM DEVELOPMENT

There are three levels of algorithms that are commonly used with the LiDAR sensors. Hardware algorithms are typically used to make the LiDAR sensors more efficient and reliable to generate raw point clouds. These are typically developed by the LiDAR sensor manufacturers. Perception and classification algorithms are used to cluster the point clouds into objects and to identify characteristics of the object (type, behaviors, etc.). These are developed by the equipment manufacturers or third-party vendors. Integration algorithms are developed for specific applications. In this study, an integration algorithm was developed to integrate the LiDAR tracking algorithm with real-time traffic signal status at intersections. The custom software that was developed to record pedestrian data from the LiDAR device recorded the following elements.

- Pedestrian phase – This is the signal phase associated with the pedestrian movement (e.g., P2, P4, P6, P8).
- Pedestrian arrival time – This is the time when the pedestrian arrives at the curb.
- Pedestrian entering time – This is the time when the pedestrian enters a zone that is used for delay time estimation.
- Pedestrian leaving time - This is the time when the pedestrian leaves the zone.
- Crossing time – This is the time that the pedestrian spends crossing.

- Perception reaction time – This is the time taken by the pedestrian to perceive the signal indication and react to it.

- Effective perception reaction time – This is the P-R time plus the walking time from where a pedestrian stands to the boundary of the waiting area (i.e., entering the intersection).

Using these elements, performance measures such as pedestrian delay were calculated. These are further described in the results section.

4.3   SITE SELECTION

The next step in the study was to select sites where a LiDAR device could be installed. The objective of data collection in the field was to test the device to assess its accuracy to detect and record pedestrian data at signalized intersections, and to determine whether this device can be successfully installed in the field to monitor pedestrian and vehicular movements and interact with the signal controller to dynamically impact signal operations.

Two sites were selected for data collection. These sites were selected in consultation with the staff at the cities of Arlington and Irving, TX. The first site was at W. Walnut Hill Lane and N. Belt Line Road. This site is in Irving, TX, and is close to the Dallas Fort Worth International Airport. W. Walnut Hill Lane in the eastbound direction has two left-turn lanes, one thru lane and one shared thru/right-turn lane. In the westbound direction, there is one left-turn lane, two thru lanes and one shared thru/right-turn lane. There are four crosswalks at this intersection corresponding with phases 2, 4, 6 and 8, as shown in Figure 4.1.

The second intersection that was selected was located at the intersection of UTA Boulevard and S. Cooper Street in Arlington, TX. This location is located on the University of Texas at Arlington's campus and is right next to the engineering building. As such, it was expected to have large pedestrian volumes when the university is in session. Figure 4.1 shows the satellite view of the UTA Boulevard and S. Cooper Street intersection. UTA Boulevard in the east and westbound directions has one left-turn lane, one thru lane, one pocket bike lane and one right-turn lane. S. Cooper Street in the northbound direction has

one left-turn lane, two thru lanes and one right-turn lane, while in the southbound direction there is one left-turn lane, two thru lanes and one shared thru/right-turn lane. There are four crosswalks at this intersection corresponding with phases 2, 4, 6 and 8, as shown in Figure 4.1.
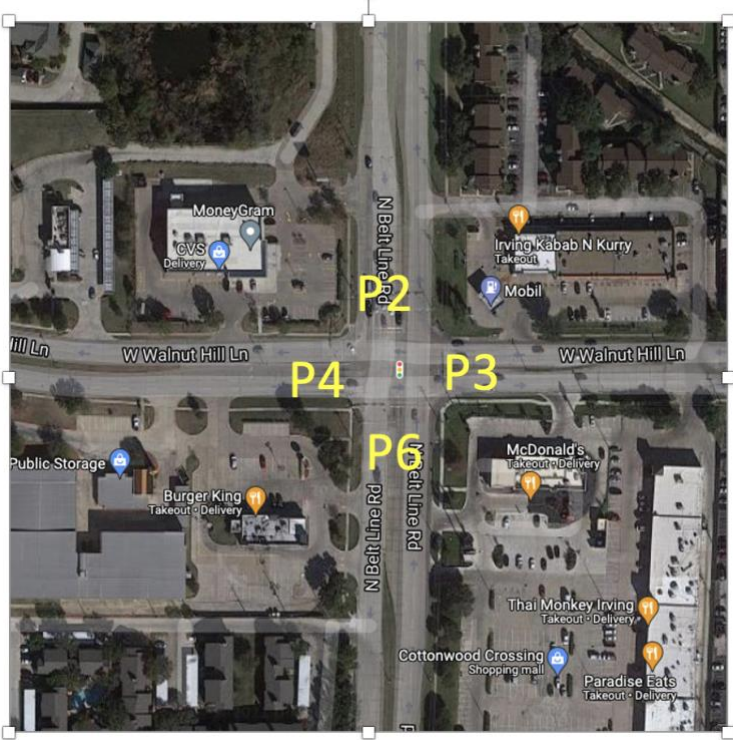
Figure 4.2: W. Walnut Hill Lane and N. Belt Line Road.

Figure 4.3: UTA Boulevard and S. Cooper Street.

4.4 DATA COLLECTION

Four LiDAR devices were set up at each of the selected intersections on the mast arm. The data from these devices was transmitted to a LiDAR hub node from which it was retrieved and used for further analysis. Collection of data at W. Walnut Hill Lane and N. Beltline Road started on 12/12/20 and 10/31/21. There were a number of data gaps observed, possibly because the device was disconnected. A total of 4,289 observations were recorded at this intersection. However, for some records the arrival time, entering time and/or leaving time were not recorded in the data, perhaps due to the pedestrian stepping outside the zone that was drawn to record these metrics. In such cases, these incomplete records were discarded, which resulted in 3,524 pedestrian observations. These were used for further analysis. Data collection at the intersection of UTA Boulevard and S. Cooper Street on 7/7/21 and ended on 12/6/21. At this intersection, 50,250 pedestrian observations were recorded at all four crosswalks. After removal of incomplete records, 50,167 pedestrian observations were retained for further analysis.

4.5 RESULT ANALYSIS

Figures 4.4 and 4.5 show the number of observed pedestrians by month and phase at the two sites. The total number of pedestrians observed were three at 524 at W. Walnut Hill Lane and N. Beltline Road, and 50,167 pedestrians were observed at UTA Boulevard and S. Cooper Street across all crosswalks and phases. As stated previously, data gaps were observed at the W. Walnut Hill Lane and N. Beltline Road Intersection, as also seen in Figure 4.4, with the largest data gap observed between July and September. More pedestrians were observed on the crosswalk associated with phase 3, which is the east crosswalk on W. Walnut Hill Lane. At the UTA Boulevard and S. Cooper Street intersection, observed pedestrian volumes increased between July and October, with the highest observations recorded in October in the crosswalk associated with phase 4. This is the north crosswalk on S. Cooper Street.
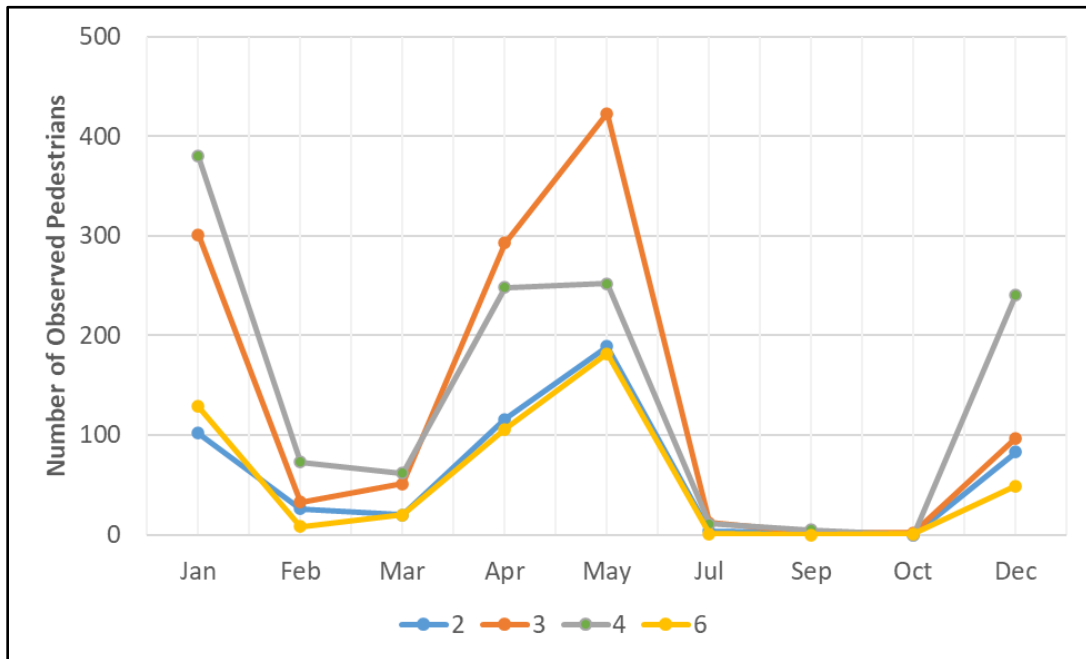
Figure 4.4: Number of pedestrians observed per phase and month at W. Walnut Hill Lane and N. Beltline Road.
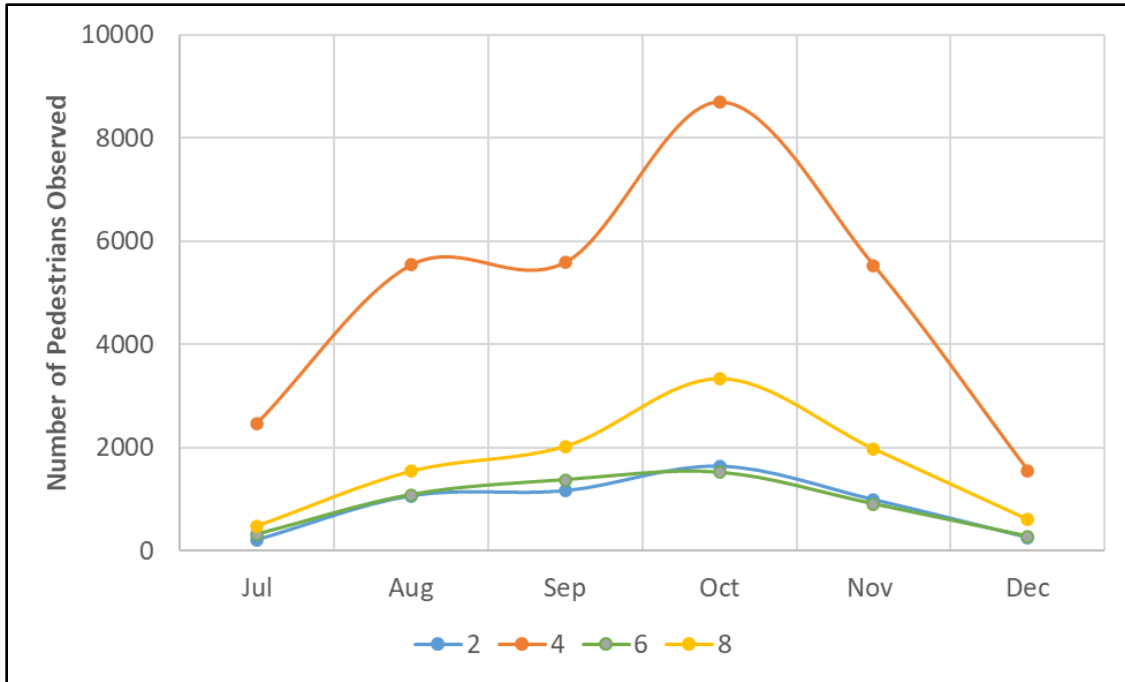
Figure 4.5: Number of pedestrians observed per phase and month at UTA Boulevard and S. Cooper Street.

Tables 4-1 and 4-2 show the various pedestrian performance metrics collected at the two intersections. At the W. Walnut Hill Lane and N. Beltline Road intersection, the average effective perception reaction time varied between 5.3 seconds for phase 6 to 6.7 seconds for phase 2. These observed values are significantly higher than those reported in the literature. Wood et al. recruited eight participants to jog and walk across the intersection and found that the perception reaction time between the auditory signal onset to the end of the forward motion varies between 0.9 seconds to 1.9 seconds, with a mean of 1.23 seconds (Wood et al., 2010). Fogger et al. studied the perception reaction time depending on the level of anticipation, which was categorized into pedestrians who were looking directly at the WALK signal, pedestrians who were anticipating crossing either by watching the opposing traffic signal or the flow of traffic, and pedestrians who were distracted in some way (Fogger et al., 2000). Younger pedestrians (< 55 years of age) tended to have shorter perception-reaction times than older pedestrians (> 55 years of age). The perception-reaction times for pedestrians looking straight ahead at the WALK signal was 0.84 $\pm$ $\pm$0.51s, 0.77 $\pm$ 0.75s for those anticipating a light change and 1.87 $\pm$

1.0 seconds for distracted pedestrians (Fogger et al., 2000). Average crossing times varied between 16.9 seconds to 20.4 seconds, while average pedestrian delay varied between 28.4 seconds and 43.6 seconds.

The perception-reaction times at the intersection of UTA Boulevard and S. Cooper Street varied between 1.7 seconds to 2.8 seconds, with an average of 2.1 seconds, which is more in line with values seen in the literature. Audible pedestrian signals (APS) are present at this intersection, which also serve to alert pedestrians to any change in signal display, thus lowering their perception-reaction times. Crossing times varied between 11.2 seconds and 16.5 seconds with an average of 15.5 seconds, while pedestrian delays varied between 32.2 seconds and 48.7 seconds with an average of 44.8 seconds.

Table 4-1: Pedestrian performance metrics at W. Walnut Hill Lane and N. Beltline Road

Phase	Number of Pedestrian Observations	Average of Perception-Reaction Time (s)	Average of crossing time (s)	Average of Pedestrian Delay (s)
2	542	6.7	16.9	29.5
3	1214	5.6	20.4	43.6
4	1272	5.8	19.2	42.6
6	496	5.3	16.9	28.4
Total	**3524**	**5.8**	**18.9**	**38.9**

Table 4-2: Pedestrian performance metrics at UTA Boulevard and S. Cooper Street

Phase	Number of Pedestrian Observations	Average of Perception-Reaction Time (s)	Average of crossing time (s)	Average of Pedestrian Delay (s)
2	5326	2.2	13.0	31.6
4	29397	1.7	16.4	48.2
6	5485	2.7	11.2	32.2
8	9959	2.8	16.5	48.7

Total	50167	2.1	15.5	44.8

4.6   SUMMARY

In this project, the investigators explored the possibility of applying the LiDAR sensing technologies to pedestrian behavioral data collection and safety protection. Through a customized solution, the investigators synchronized the pedestrian behaviors with the traffic signal status. The pedestrian behavioral data showed that the ADA-compliant pedestrian push buttons can significantly reduce pedestrians' perception-reaction time to a WALK signal.

In addition, the investigators also explored a novel dynamic flashing yellow arrow mechanism based on pedestrian tracking. The D-FYA aims to separate permissive left-turn vehicles from the concurrent crossing pedestrians. The simulation results were promising and the D-FYA will proceed to the field test in the future. The investigators also designed a three-color code to demonstrate the pedestrian behaviors.

The findings will benefit the pedestrian safety improvement.

5.0 REFERENCES

- American Association of State Highway Officials, National Conference on Street and Highway Safety, 1935. Manual of Uniform Traffic Control Devices for Streets and Highways, 1935th ed. Public Roads Administration.
- Barlow, J., Bentzen, B., Tabor, L., 2003. Accessible Pedestrian Signals: Synthesis and Guide to Best Practice.
- Federal Highway Administration, 2016. Traffic MonitoringGuide.
- Garcia, F., Jiménez, F., Naranjo, E., Zato, J., Aparicio, F., Armingol, J., de la Escalera, A., 2009. Analysis of LIDAR sensors for new ADAS applications. Usability in moving obstacles detection. Presented at the 16th ITS World Congress and Exhibition on IntelligentTransportation Systems and Services, Stockholm, Sweden.
- Grembek, O., 2019. The Safe System Approach: Considertions for Developing a Multi-Layered System.
- Gutfreund, O.D., 2004. Twentieth century sprawl: highways and the reshaping of the American Landscape. Oxford University Press, New York.
- Hassan, S.A., Hounsell, N.B., Shrestha, B.P., 2017. Investigating the Applicability of Upstream Detection Strategy at Pedestrian Signalised Crossings. PROMET 29, 503–510. https://doi.org/10.7307/ptt.v29i5.2225
- Heuel, S., Rohling, H., 2012. Pedestrian classification in automotive radar systems, in: 2012 13th International Radar Symposium. Presented at the 2012 13th International Radar Symposium (IRS), IEEE, Warsaw, Poland, pp. 39–44. https://doi.org/10.1109/IRS.2012.6233285
- Hou, Y., Sun, C., Edara, P., 2012. Statistical Test for 85th and 15th Percentile Speeds with Asymptotic Distribution of Sample Quantiles. Transportation Research Record 2279, 47–53. https://doi.org/10.3141/2279-06
- Hughes, R., Huang, H., Zeeger, C., Cynecki, M., 2001. Evaluation of Automated Pedestrian Detection at Signalized Intersections. Publication FHWA-RD-00-097, FHWA, U.S. Department of Transportation, 2001 (No. FHWA-RD-00-097). USDOT FHWA.
- Hyun, E., Jin, Y.-S., Lee, J.-H., 2016. A Pedestrian Detection Scheme Using a Coherent Phase Difference Method Based on 2D Range-Doppler FMCW Radar. Sensors 16, 124. https://doi.org/10.3390/s16010124
- Institute of Electrical and Electronics Engineers, IEEE Aerospace and Electronic Systems Society (Eds.), 2010. 2010 IEEE Radar Conference: Arlington, Virginia, USA, 10 - 14 May 2010. Presented at the IEEE International Radar Conference, IEEE, Piscataway, NJ.
- Institute of Transportation Engineers (Ed.), 2004. Toolbox on intersection safety and design. Institute of Transportation Engineers, Washington, D.C.
- Institute of Transportation Engineers, 1998. Design and safety of pedestrian facilities, an ITE recommended practice.
- Kilambi, P., Ribnick, E., Joshi, A.J., Masoud, O., Papanikolopoulos, N., 2008. Estimating pedestrian counts in groups. Computer Vision and Image Understanding 110, 43–59. https://doi.org/10.1016/j.cviu.2007.02.003

- Kim, G., Park, Y., 2016. LIDAR pulse coding for high resolution range imaging at improved refresh rate. Opt. Express 24, 23810. https://doi.org/10.1364/OE.24.023810
- Klein, L., Mills, M., Glbson, D., Turner-Fairbank Highway Research Center, 2006. Traffic Detector Handbook: Third Edition--Volume I (Tech Report No. FHWA-HRT-06-108).
- Kothuri, S., Nordback, K., Schrope, A., Phillips, T., Figliozzi, M., 2017. Bicycle and Pedestrian Counts at Signalized Intersections Using Existing Infrastructure: Opportunities and Challenges. Transportation Research Record 2644, 11–18. https://doi.org/10.3141/2644-02
- Larson, T., 2020. Evaluation of Dynamic Passive Pedestrian Detection with a Framework for Future Applications. Oregon State University.
- Levinson, D.M., Krizek, K.J., 2008. Planning for place and plexus: metropolitan land use and transport. Routledge, New York ; London.
- Li, S., Sayed, T., Zaki, M.H., Mori, G., Stefanus, F., Khanloo, B., Saunier, N., 2012. Automated Collection of Pedestrian Data through Computer Vision Techniques. Transportation Research Record 2299, 121–127. https://doi.org/10.3141/2299-13
- Manston, K., 2011. The Challenges of Using Radar for Pedestrian Detection. Siemens.
- Marisamynathan, Perumal, V., 2014. Study on pedestrian crossing behavior at signalized intersections. Journal of Traffic and Transportation Engineering (English Edition) 1, 103–110. https://doi.org/10.1016/S2095-7564(15)30094-5
- McGee, H., Moriarty, K., Gates, T.J., 2012. Guidelines for Timing Yellow and Red Intervals at Signalized Intersections. Transportation Research Record 2298, 1–8. https://doi.org/10.3141/2298-01
- Noyce, D.A., Bentzen, B.L., 2005. Determination of Pedestrian Push-Button Activation Duration at Typical Signalized Intersections. Transportation Research Record 1939, 63–68. https://doi.org/10.1177/0361198105193900108
- Ozbay, K., Bartin, B., Yang, H., Walla, R., Williams, R., 2010. Automatic Pedestrian Counter (No. FHWA-NJ-2010-001). Rutgers University.
- Schad, B., 1935. Traffic Control at Signalized Street Intersections. University of Michigan.
- Schultz, G., Berret, J., Eggest, D., 2019. Pedestrian walking speeds at signalized interiections in Utah (No. UT-19.06). Bringham Young University.
- Thakur, R., 2016. Scanning LIDAR in Advanced Driver Assistance Systems and Beyond: Building a road map for next-generation LIDAR technology. IEEE Consumer Electron. Mag. 5, 48–54. https://doi.org/10.1109/MCE.2016.2556878
- Turley, J., 2018. Cepton LiDAR Goes Anti-MEMS Route. Electronic Engineering Journal, Techfocus Media.
- Williams, G.M., 2017. Optimization of eyesafe avalanche photodiode LiDAR for automobile safety and autonomous navigation systems. Opt. Eng 56, 031224. https://doi.org/10.1117/1.OE.56.3.031224
- Yang, H., Ozbay, K., Bartin, B., 2011. Enhancing the Quality of Infrared-Based Automatic Pedestrian Sensor Data by Nonparametric Statistical Method. Transportation Research Record 2264, 11–17. https://doi.org/10.3141/2264-02

- Zeegeer, C., Semler, C., Sanders, M., Steyn, H., Ryus, P., Hunter, W.W., Koonce, P., 2020. Guidance to improve pedestrian and bicyclist safety at intersections: <br>, National cooperative highway research program research report. Transportation Research Board, Washington.
- Baek, J., Hong, S., Kim, J., and Kim, E. (2017). "Efficient pedestrian detection at nighttime using a thermal camera." Sensors, 17(8), 1850.
- Bhuvaneshwar, V., and Mirchandani, P. B. "Real-time detection of crossing pedestrians for traffic-adaptive signal control." Proc., Proceedings. The 7th International IEEE Conference on Intelligent Transportation Systems (IEEE Cat. No. 04TH8749), IEEE, 309-313.
- Bu, F., Le, T., Du, X., Vasudevan, R., and Johnson-Roberson, M. (2019). "Pedestrian Planar LiDAR Pose (PPLP) Network for Oriented Pedestrian Detection Based on Planar LiDAR and Monocular Images." IEEE Robotics and Automation Letters, 5(2), 1626-1633.
- Chan, A. B., Liang, Z.-S. J., and Vasconcelos, N. "Privacy preserving crowd monitoring: Counting people without people models or tracking." Proc., 2008 IEEE Conference on Computer Vision and Pattern Recognition, IEEE, 1-7.
- Chan, A. B., and Vasconcelos, N. "Bayesian poisson regression for crowd counting." Proc., 2009 IEEE 12th international conference on computer vision, IEEE, 545-551.
- Combs, T. S., Sandt, L. S., Clamann, M. P., and McDonald, N. C. (2019). "Automated vehicles and pedestrian safety: exploring the promise and limits of pedestrian detection." American journal of preventive medicine, 56(1), 1-7.
- El Ansari, M., Lahmyed, R., and Trémeau, A. "A Hybrid Pedestrian Detection System based on Visible Images and LIDAR Data." Proc., VISIGRAPP (5: VISAPP), 325-334.
- Grassi, A. P., Frolov, V., and León, F. P. (2011). "Information fusion to detect and classify pedestrians using invariant features." Information fusion, 12(4), 284-292.
- John, V., Tsuchizawa, S., Liu, Z., and Mita, S. (2017). "Fusion of thermal and visible cameras for the application of pedestrian detection." Signal, Image and Video Processing, 11(3), 517-524.
- Kilambi, P., Ribnick, E., Joshi, A. J., Masoud, O., and Papanikolopoulos, N. (2008). "Estimating pedestrian counts in groups." Computer Vision and Image Understanding, 110(1), 43-59.
- Kim, J. "Pedestrian Detection and Distance Estimation Using Thermal Camera in Night Time." Proc., 2019 International Conference on Artificial Intelligence in Information and Communication (ICAIIC), IEEE, 463-466.
- Kothuri, S., Nordback, K., Schrope, A., Phillips, T., and Figliozzi, M. (2017). "Bicycle and pedestrian counts at signalized intersections using existing infrastructure: opportunities and challenges." Transportation research record, 2644(1), 11-18.
- Li, B., Yao, Q., and Wang, K. "A review on vision-based pedestrian detection in intelligent transportation systems." Proc., Proceedings of 2012 9th IEEE international conference on networking, sensing and control, IEEE, 393-398.
- Lv, B., Sun, R., Zhang, H., Xu, H., and Yue, R. (2019). "Automatic Vehicle-Pedestrian Conflict Identification With Trajectories of Road Users Extracted From Roadside LiDAR Sensors Using a Rule-Based Method." IEEE Access, 7, 161594-161606.
- Manston, K. (2011). "The challenges of using radar for pedestrian detection." Traffic Engineering & Control, 52(7).

- National Highway Traffic Safety Administration (2020). "Overview of motor vehicle crashes in 2019." US Department of Transportation: Washington, DC, USA.
- National Highway Traffic Safety Administration (2020). "Traffic Safety Facts 2020 Data" Accessed from https://crashstats.nhtsa.dot.gov/Api/Public/ViewPublication/813310
- Noyce, D. A., Bill, A. R., and Knodler Jr, M. A. (2014). "Evaluation of the Flashing Yellow Arrow (FYA) Permissive Left-Turn in Shared Yellow Signal Sections."
- Soundrapandiyan, R., and Mouli, P. C. (2015). "Adaptive pedestrian detection in infrared images using background subtraction and local thresholding." Procedia Computer Science, 58(1), 706-713.
- Tang, S., Ye, M., Zhu, C., and Liu, Y. (2017). "Adaptive pedestrian detection using convolutional neural network with dynamically adjusted classifier." Journal of Electronic Imaging, 26(1), 013012.
- Wu, J., Xu, H., Sun, Y., Zheng, J., and Yue, R. (2018). "Automatic background filtering method for roadside LiDAR data." Transportation Research Record, 2672(45), 106-114.
- Yoshinaga, S., Shimada, A., and Taniguchi, R.-i. (2010). "Real-time people counting using blob descriptor." Procedia-Social and Behavioral Sciences, 2(1), 143-152.
- Zhao, H., Sha, J., Zhao, Y., Xi, J., Cui, J., Zha, H., and Shibasaki, R. (2011). "Detection and tracking of moving objects at intersections using a network of laser scanners." IEEE transactions on intelligent transportation systems, 13(2), 655-670.
- Zhao, H., and Shibasaki, R. (2005). "A novel system for tracking pedestrians using multiple single-row laser-range scanners." IEEE Transactions on systems, man, and cybernetics-Part A: systems and humans, 35(2), 283-291.
- Zhao, J., Li, Y., Xu, H., and Liu, H. (2019). "Probabilistic prediction of pedestrian crossing intention using roadside LiDAR data." IEEE Access, 7, 93781-93790.
- Zhao, J., Xu, H., Wu, J., Zheng, Y., and Liu, H. (2019). "Trajectory tracking and prediction of pedestrian's crossing intention using roadside LiDAR." IET Intelligent Transport Systems, 13(5), 789-795.